Electronic Supporting Information for

Mechanistic and kinetic studies of the direct alkylation of benzylic amines – A formal C(sp^3)-H activation proceeds actually via a C(sp^2)-H activation pathway

*Robert Pollice, Navid Dastbaravardeh,† Nada Marquise, Marko D. Mihovilovic, and Michael Schnürch**

Institute of Applied Synthetic Chemistry, Vienna University of Technology, Getreidemarkt 9/163-OC, Vienna 1060, Austria

Table of Contents

1. General methods

In general, unless noted otherwise, chemicals were purchased from commercial suppliers and used without further purification. Toluene (99.85 %, AcroSeal) was used without further purification. O-xylene (≥98 %, Fluka) was dried over molecular sieves (4 Å) prior to use. All benzylic amines used as starting materials for C-H activation reactions were synthesized according to literature procedures. Compounds **1**[1], **1a**[1], **1c**[1], **7a**[1], **7b**[1] and **9**[2] were synthesized according to literature procedures. Cyclooctadiene rhodium chloride dimer (98 %, Strem) was generally handled in a glove box under argon. 1-Bromohexane was distilled under reduced pressure prior to use.

Water contents of K_2CO_3 batches were determined by measuring the loss on heating of the corresponding solids by heating them to about 200 °C under medium vacuum overnight assuming that only water was lost in the process. The same procedure was followed to obtain dry potassium carbonate. Amounts of potassium carbonate and caesium carbonate were calculated assuming the solid to be completely dry, unless noted otherwise.

^{1}H-NMR and ^{13}C-NMR spectra were recorded on either a *Bruker Avance 200* or a *Bruker Avance 400*, chemical shifts are reported in ppm, using Me_4Si as internal standard and, unless noted otherwise, $CDCl_3$ as solvent.

GC-MS was performed on a *Thermo Fischer GC Focus/ MS DSQ II (quadrupole, EI+)* with a BGB5 column (30 m · 0.32 mm, 1.0 µm film, achiral).

GC measurements were carried out on a Thermo Focus GC using a BGB-5 (30 m x 0.32 mm, 1.0 µm film, achiral, 5% diphenylpolysiloxane, 95% dimethylpolysiloxane) capillary column. The oven temperature program used was 100 °C (2 min), 18 °C · min^{-1}, 280 °C (5 min). GC yields were calculated by using the conversion factor of the corresponding compound relative to dodecane as internal standard which was determined by calibration.

For TLC aluminium backed silica gel 60 with fluorescence indicator F_{254} was used. Column chromatography was performed on Silica 60 from Merck (40-63 µm) unless noted otherwise. Flash chromatography, unless noted otherwise, was carried out on a Büchi Sepacore™ MPLC system.

Melting points were determined on an automated melting point system (BÜCHI Melting Point B-545) and are uncorrected.

IR measurements for quantification were carried out on a *PerkinElmer Spectrum 400* in transmission mode using a ZnSe cuvette. ATR-IR measurements for characterization were carried out on a *PerkinElmer Spectrum 65*. IR spectra were recorded as average over 16 spectra, the resolution of the recorded spectra was 4 cm^{-1}.

High-resolution mass spectrometry (HRMS) for literature-unknown compounds was performed by liquid chromatography in combination with hybrid ion trap and high-resolution time-of-flight mass spectrometry (LC-IT-TOF-MS) in only positive-ion detection mode with the recording of standard (MS) and tandem (MS/MS) spectra.

2. Experimental procedures

2.1 General procedure I for C-H activation reactions

Solid and non-volatile liquid starting materials were placed in an oven-dried 8 ml vial with a septum screw cap and a magnetic stirring bar. The vial was evacuated and flushed with argon three times. Liquid starting materials and solvent were added via syringe through septum. Finally, the vial was closed with a fully covered solid Teflon-lined cap. The reaction mixture was heated in a reaction block at the desired temperature for the desired reaction time.

2.2 General procedure II for C-H activation reactions

Solid and non-volatile liquid starting materials except catalyst were placed in an oven-dried 8 ml vial with a fully covered solid Teflon-lined cap and a magnetic stirring bar under ambient atmosphere. The vial was transferred into a glove-box under argon. Catalyst, liquid starting materials and solvent were added inside the glove-box. Finally, the vial was closed and the reaction mixture was heated in a reaction block at the desired temperature for the desired reaction time.

2.3 General work-up procedure for C-H activation reactions

After cooling the reaction mixture to room temperature the solid material was removed by filtration and washed with CH_2Cl_2. The combined organic filtrate was concentrated in vacuo and the resulting crude residue was purified by flash column chromatography [petroleum ether/ethyl acetate (PE/EtOAc)].

2.4 Optimization studies for the direct alkylation of benzylic amine with alkyl bromide

All experiments were carried out according to general procedure I on a 0.5 mmol scale with a concentration of 0.25 mol/l of benzylamine **1** in the corresponding solvent. The following table shows some selected results of the optimization studies carried out.

Table S1. Screening results for direct C-H alkylation of **1** using alkyl bromides.

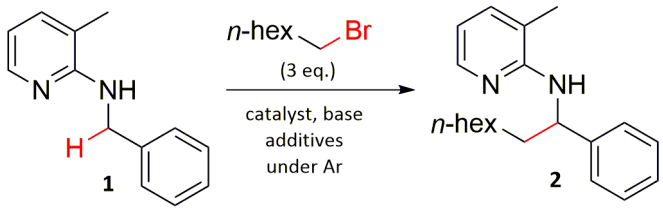

Entry	Catalyst[a]	Base	Additive	Solvent	Temperature[b]	Time	Conversion[c] of 1	Conversion[c] to 2
1	$[RuCl_2(p\text{-cymene})]_2$ (0.1 eq.)	K_2CO_3 (3 eq.)	PPh_3 (0.05 eq.) cyclohexanol (1 eq.)	*o*-xylene	140 °C	24 h	56%	23%
2	$[RuCl_2(p\text{-cymene})]_2$ (0.1 eq.)	K_2CO_3 (3 eq.)	KOPiv (0.3 eq.) cyclohexanol (1 eq.)	*o*-xylene	140 °C	24 h	60%	20%
3	$[RuCl_2(p\text{-cymene})]_2$ (0.1 eq.)	K_2CO_3 (3 eq.)	cyclohexanol (1 eq.)	*o*-xylene	140 °C	24 h	40%	4%
4	$[RuCl_2(p\text{-cymene})]_2$ (0.1 eq.)	K_2CO_3 (3 eq.)	PPh_3 (0.05 eq.) cyclohexanol (1 eq.)	*o*-xylene	100 °C	24 h	22%	3%
5	$[RuCl_2(p\text{-cymene})]_2$ (0.1 eq.)	K_2CO_3 (3 eq.)	PPh_3 (0.05 eq.) cyclohexanol (1 eq.)	*o*-xylene	120 °C	24 h	29%	5%
6	$[RuCl_2(p\text{-cymene})]_2$ (0.1 eq.)	K_2CO_3 (3 eq.)	PPh_3 (0.05 eq.) cyclohexanol (1 eq.)	*o*-xylene	130 °C	24 h	50%	16%
7	$[RuCl_2(p\text{-cymene})]_2$ (0.1 eq.)	K_2CO_3 (3 eq.)	PPh_3 (0.05 eq.) cyclohexanol (1 eq.)	*o*-xylene	150 °C	24 h	73%	25%
8	$[RuCl_2(p\text{-cymene})]_2$ (0.1 eq.)	K_2CO_3 (3 eq.)	PPh_3 (0.05 eq.) cyclohexanol (1 eq.)	*o*-xylene	160 °C	24 h	76%	23%
9	$[RuCl_2(benzene)]_2$ (0.1 eq.)	K_2CO_3 (3 eq.)	cyclohexanol (1 eq.)	*o*-xylene	140 °C	24 h	40%	4%
10	$[RuCl_2(cod)]_n$ (0.1 eq.)	K_2CO_3 (3 eq.)	cyclohexanol (1 eq.)	*o*-xylene	140 °C	24 h	73%	27%

11	$[RhCl(cod)]_2$ (0.1 eq.)	K_2CO_3 (3 eq.)	cyclohexanol (1 eq.)	*o*-xylene	140 °C	24 h	70%	31%
12	$[RhCp^*Cl_2]_2$ (0.1 eq.)	K_2CO_3 (3 eq.)	cyclohexanol (1 eq.)	*o*-xylene	140 °C	24 h	31%	2%
13	Rh_4CO_{12} (0.025 eq.)	K_2CO_3 (3 eq.)	cyclohexanol (1 eq.)	*o*-xylene	140 °C	24 h	11%	<1%
14	$[RuCl_2(cod)]_n$ (0.1 eq.)	K_2CO_3 (3 eq.)	PPh_3 (0.05 eq.) cyclohexanol (1 eq.)	*o*-xylene	140 °C	24 h	53%	20%
15	$[RhCl(cod)]_2$ (0.1 eq.)	K_2CO_3 (3 eq.)	PPh_3 (0.05 eq.) cyclohexanol (1 eq.)	*o*-xylene	140 °C	24 h	40%	9%
16	$[RuCl_2(cod)]_n$ (0.1 eq.)	K_2CO_3 (3 eq.)	KOPiv (0.3 eq.) cyclohexanol (1 eq.)	*o*-xylene	140 °C	24 h	64%	20%
17	$[RhCl(cod)]_2$ (0.1 eq.)	K_2CO_3 (3 eq.)	KOPiv (0.3 eq.) cyclohexanol (1 eq.)	*o*-xylene	140 °C	24 h	65%	25%
18	$[RhCl(cod)]_2$ (0.1 eq.)	K_2CO_3 (3 eq.)	cyclohexanol (1 eq.)	toluene	140 °C	24 h	73%	37%
19	$[RhCl(cod)]_2$ (0.1 eq.)	K_2CO_3 (3 eq.)	cyclohexanol (1 eq.)	toluene	160 °C	24 h	97%	70% (56%)[d]
20	$[RhCl(cod)]_2$ (0.1 eq.)	K_2CO_3 (3 eq.)	-	toluene	160 °C	24 h	98%	70%
21	$[RuCl_2(cod)]_n$ (0.1 eq.)	K_2CO_3 (3 eq.)	cyclohexanol (1 eq.)	toluene	160 °C	24 h	92%	59%
22	$[RuCl_2(cod)]_n$ (0.1 eq.)	K_2CO_3 (3 eq.)	-	toluene	160 °C	24 h	100%	46%
23	$[RhCl(cod)]_2$ (0.1 eq.)	K_2CO_3 (3 eq.)	-	*o*-xylene	160 °C	24 h	95%	64%
24	$[RhCl(cod)]_2$ (0.1 eq.)	Cs_2CO_3 (3 eq.)	cyclohexanol (1 eq.)	toluene	160 °C	24 h	75%	49%
25	$[RhCl(cod)]_2$ (0.1 eq.)	Cs_2CO_3 (3 eq.)	-	toluene	160 °C	24 h	87%	59%

a) Equivalents based on monomer unit.

b) Reaction block temperatures and not inside temperatures of the reaction mixtures.

c) Based on GC analysis of the reaction mixture with dodecane as internal standard.

d) Isolated yield

N-(1-phenyloctyl)-3-methylpyridin-2-amine (2):

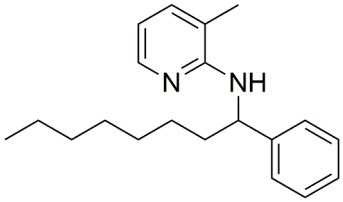

The reaction was carried out according to general procedure I with **1** (99 mg, 0.5 mmol, 1 eq.), 1-bromoheptane (269 mg, 1.5 mmol, 3 eq.), K_2CO_3 (207 mg, 1.5 mmol, 3 eq.), $[RhCl(cod)]_2$ (12 mg, 0.025 mmol, 0.05 eq.) and cyclohexanol (50 mg, 0.5 mmol, 1 eq.) in dry toluene (2 ml). The reaction mixture was heated for 24h at 160 °C. The general work-up procedure for C-H activation reactions was followed (PE/EtOAc 99:1). Yellowish oil (83 mg, 56% yield). ^{1}H-NMR ($CDCl_3$, 200 MHz): δ = 0.85 (t, J = 6.8 Hz, 3 H), 1.08-1.51 (m, 10 H), 1.71-1.99 (m, 2 H), 2.09 (s, 3 H), 4.36 (d, J = 7.6 Hz, 1 H), 5.23 (q, J = 7.4 Hz, 1 H), 6.45 (dd, J = 7.0, 5.1 Hz, 1 H), 7.03-7.43 (m, 6 H), 7.95 (dd, J = 5.1, 1.6 Hz, 1H) ppm. ^{13}C-NMR ($CDCl_3$, 50 MHz): δ = 14.1, 17.1, 22.7, 26.4, 29.2, 29.6, 31.8, 37.6, 54.7, 112.5, 116.2, 126.5, 126.7, 128.4, 136.8, 144.6, 145.5, 156.2 ppm. HRMS: calculated for $C_{20}H_{29}N_2$ $[M + H]^+$ 297.2325; found 297.2325.

2.5 Substrate scope investigation for the direct alkylation of benzylic amine

Experiments were carried out according to the reaction conditions from the experiment corresponding to entry 14 of the optimization studies. Products were isolated using the general work-up procedure for C-H activation reactions. It should be noted that these experiments were single experiments and the low yield with the secondary alkyl bromide could be an outlier.

Scheme S1.

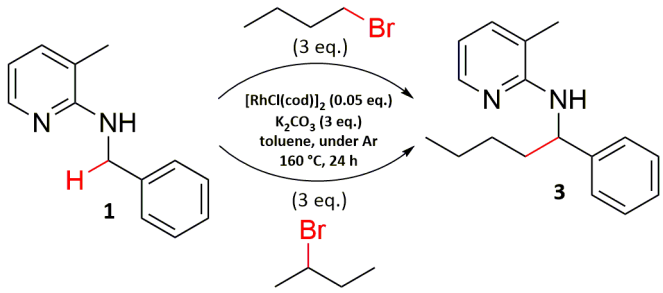

N-(1-phenylpentyl)-3-methylpyridin-2-amine (3):

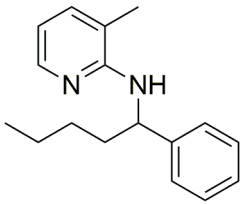

The reaction was carried out according to general procedure I with **1** (99 mg, 0.5 mmol, 1 eq.), 1-bromobutane (206 mg, 1.5 mmol, 3 eq.), K_2CO_3 (207 mg, 1.5 mmol, 3 eq.), $[RhCl(cod)]_2$ (12 mg, 0.025 mmol, 0.05 eq.) and cyclohexanol (50 mg, 0.5 mmol, 1 eq.) in dry toluene (2 ml). The reaction mixture was heated for 24h at 160 °C. The general work-up procedure for C-H activation reactions was followed (PE/EtOAc 99:1). Colorless oil (64 mg, 50% yield). ^{1}H-NMR ($CDCl_3$, 200 MHz): δ = 0.87 (t, J = 6.7 Hz, 3 H), 1.16-1.49 (m, 4 H), 1.71-1.99 (m, 2 H), 2.10 (s, 3 H), 4.37 (d, J = 7.5 Hz, 1 H), 5.23 (q, J = 7.4 Hz, 1 H), 6.45 (dd, J = 7.1, 5.1 Hz, 1 H), 7.15-7.39 (m, 6 H), 7.95 (dd, J = 5.1, 1.4 Hz, 1H) ppm. ^{13}C-NMR ($CDCl_3$, 50 MHz): δ = 14.0, 17.1, 22.7, 28.5, 37.3, 54.6, 112.5, 116.1, 126.5, 126.7, 128.4, 136.7, 144.6, 145.6, 156.2 ppm. HRMS: calculated for $C_{17}H_{23}N_2$ $[M + H]^+$ 255.1856; found 255.1853.

The reaction was carried out according to general procedure I with **1** (99 mg, 0.5 mmol, 1 eq.), 2-bromobutane (206 mg, 1.5 mmol, 3 eq.), K_2CO_3 (207 mg, 1.5 mmol, 3 eq.), $[RhCl(cod)]_2$ (12 mg, 0.025 mmol, 0.05 eq.) and cyclohexanol (50 mg, 0.5 mmol, 1 eq.) in dry toluene (2 ml). The reaction mixture was heated for 24 h at 160 °C. The general work-up procedure for C-H activation reactions was followed (PE/EtOAc 99:1). Colorless oil (16 mg, 12% yield). In addition a

considerable amount of **1** was recovered (35 mg, 36% yield).

2.6 Optimized conditions for the direct alkylation of benzylic amine with alkene

This experiment was carried out according to general procedure I on a 0.25 mmol scale with a concentration of 0.25 mol/l of the benzylamine **1** in the corresponding solvent. Yields are GC yields and are based on GC analysis of the reaction mixture with dodecane as internal standard using calibration curves for products **4**, **5** and **6** to determine their concentrations.

Scheme S2.

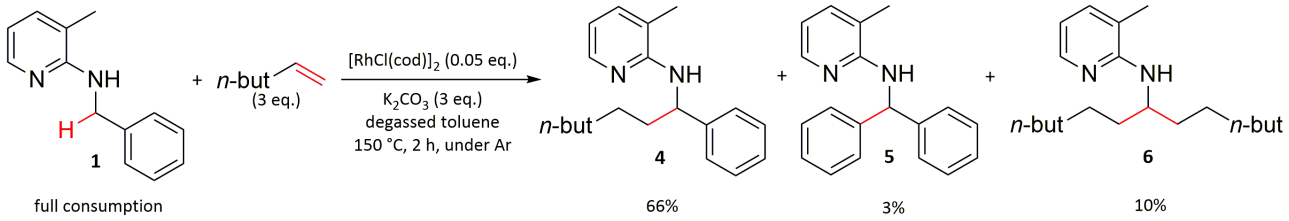

2.7 General procedure for kinetic experiments

All experiments were performed in oven-dried 8 ml vials with a fully covered solid Teflon-lined cap and a magnetic stirring bar, unless noted otherwise. Unless noted otherwise the reaction mixtures were heated in a pre-heated aluminium reaction block (150 °C) and the highest possible stirring rate (1400 rpm) on a *Heidolph MR Hei-Standard* was used. Time measurement was started immediately after placing the vials in the aluminium block. Unless noted otherwise quantifications were performed by means of GC analysis of the crude reaction mixtures using dodecane as internal standard and based on calibration curves for compounds **1**, **4**, **5** and **6** to determine their concentrations. Each kinetic experiment was performed in triplicate unless noted otherwise. GC measurements for quantifications were also performed in triplicate and the result for one sample was calculated as average over those 3 measurements and the corresponding error was calculated as standard deviation over those experiments. Given values are therefore averages over three

experiments and the corresponding error is the standard deviation over those experiments.

General procedure II for C-H activations was followed. For every individual experiment the intended amount of K_2CO_3 was placed in the vial. The vial was then transferred into a glove-box. Cyclooctadiene rhodium chloride dimer (0.0313 mol/l solution), benzylic amine derivative (0.625 mol/l solution), hex-1-ene and toluene were added in solutions inside the glove-box. Reactions were stopped by immediately cooling them down to room temperature in a water bath.

Concentrations given for K_2CO_3 are not really concentrations since it is not completely dissolved in the reaction mixture. They can be viewed as molar loading with respect to the total reaction volume. In order to estimate the total reaction volume the volumes of all solutions and the pure solvent were assumed to be additive.

2.8 Kinetic profiles

Scheme S3.

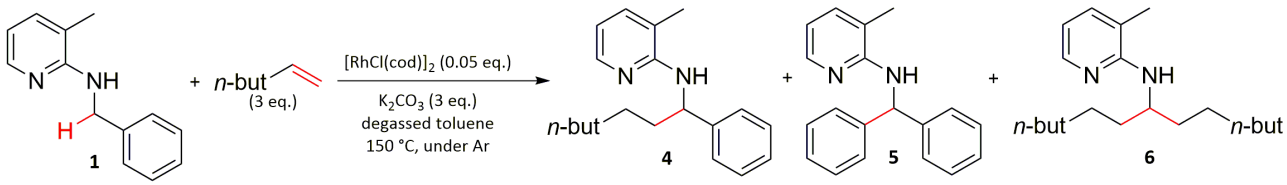

All experiments were performed according to the general procedure for kinetic experiments.

2.9 Side-product experiments

Experiments were carried out according to general procedure II and despite reaction time optimized reaction conditions for the direct alkylation of benzylic amines with alkenes were used. Yields are

based on GC analysis of the reaction mixture with dodecane as internal standard using calibration curves for compounds **1**, **4**, **5** and **6** to determine their concentrations. In general two types of experiments were performed. Either one single compound was subjected to the reaction conditions or two compounds in equal amounts were subjected to the reaction conditions.

2.10 Base studies

Scheme S4.

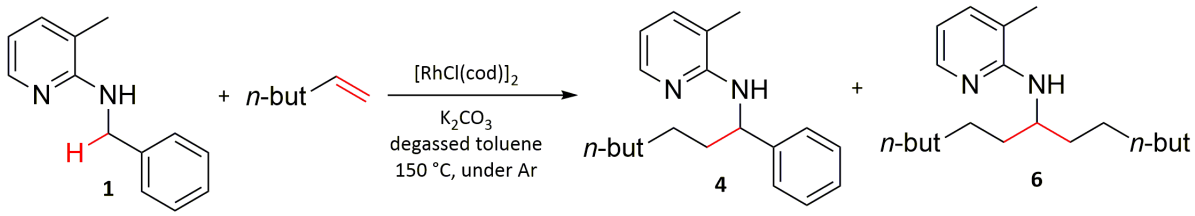

In the experiment series the influence of the water content of K_2CO_3 on the initial rate of the reaction was investigated.

2.11 Kinetic isotope effect studies

All experiments were performed according to the general procedure for kinetic experiments. KIE values were obtained by comparing the corresponding initial rates of reactions of undeuterated substrate **1** with the corresponding value with deuterated compounds.

2.12 Intermolecular KIE for benzylic C-H

Scheme S5.

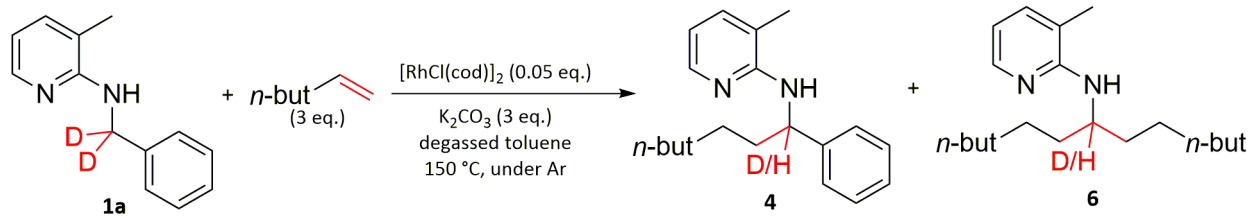

The deuterium content in the unreacted starting material was determined by ^{1}H-NMR analysis of the crude residue after filtration of the reaction mixture and evaporation of the solvent.

2.13 Intermolecular KIE for N-H

Scheme S6.

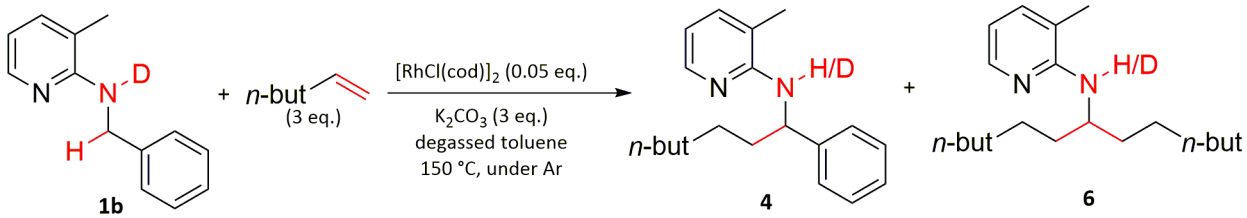

Deuterated compound **1b** was obtained by dissolving **1** in MeOD (c = 0.21 mol/l) under an inert atmosphere of argon and letting the resulting solution stand for 1 h. The solvent was removed in vacuo and the deuterated compound 1b was obtained with a typical deuterium content of 95%. IR (Transmission): $\tilde{\nu}_{N\text{-}D} = 2559\ cm^{-1}$.

The deuterium content in the unreacted starting material was determined by transmission IR analysis of the reaction mixture based on calibration curves for the N-H (3453 cm^{-1}) and the N-D (2559 cm^{-1}) bands of the starting material.

2.14 Substrate scope benzylic amine

Experiments were carried out according to general procedure II and despite reaction time optimized reaction conditions for the direct alkylation of benzylic amines with alkenes were used. In both experiments no conversion to any new product was observed neither after 3 nor after 24 h based on both GC and TLC analysis.

Scheme S7.

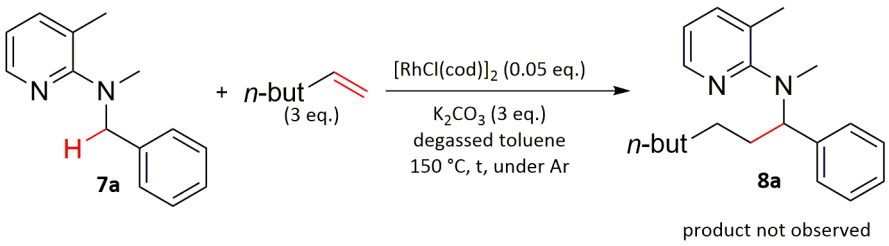

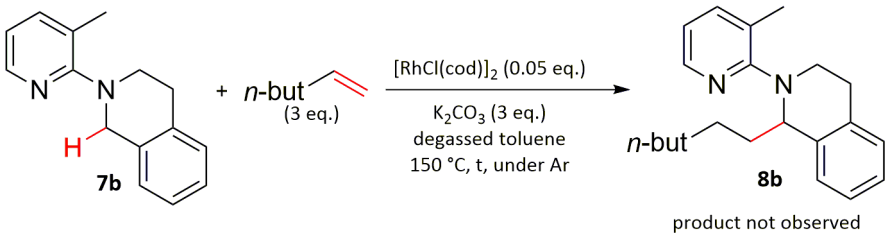

2.15 Imine experiments

Experiments were carried out according to general procedure II and in general optimized reaction conditions for the direct alkylation of benzylic amines with alkenes were used.

Scheme S8.

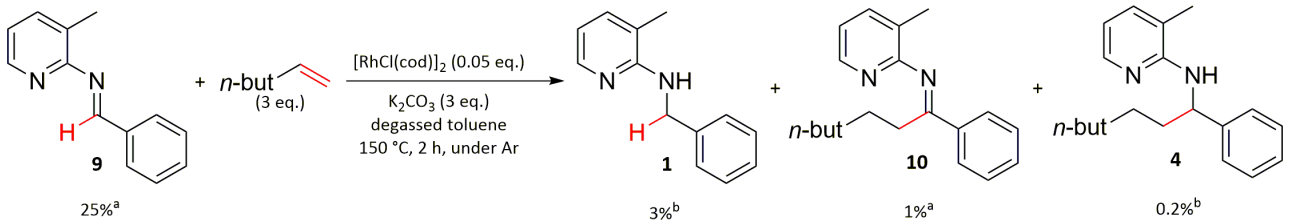

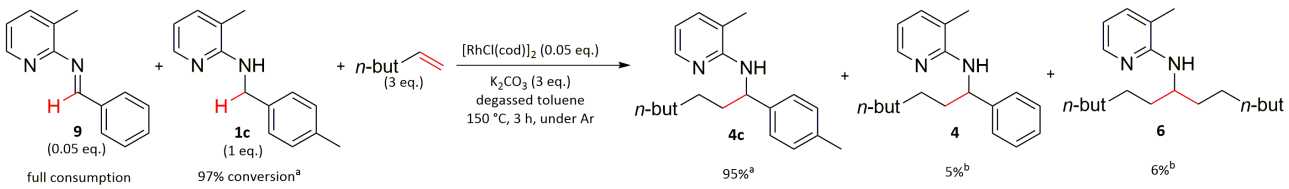

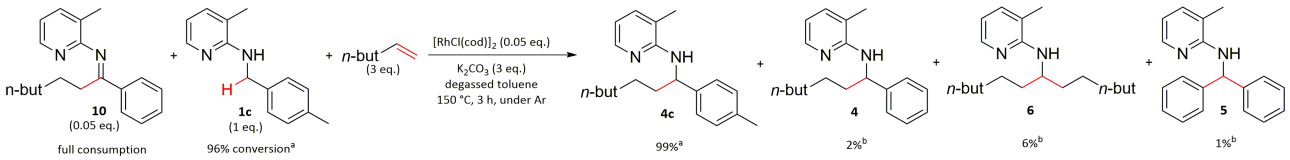

a) Based on GC analysis of the reaction mixture with dodecane as internal standard assuming a conversion factor of 1 (not calibrated).

b) Calibrated GC yields.

It was hypothesized that if imines **9** and **10** were intermediates in the reaction they should be converted to the products of the reaction under the reaction conditions. Surprisingly, by using 1 equivalent of **9** instead of **1** the reaction was significantly inhibited and only small amounts of the alkylated products **4** (about 1%) and **10** (below 1%) were observed after 2h of reaction. In addition, a small fraction of **9** was converted to the amine **1**. This result was rationalized by the imine **9** being a very strong ligand effectively coordinating multiple times to the catalytically active rhodium species thereby inhibiting the reaction.

Although compound **10** was identified as intermediate in another reaction in literature[3] it was, to the best of our knowledge, never isolated and fully characterized. The procedure was based on a literature protocol[4] but had to be modified on the basis of our protocol in order to obtain efficient conversion to the desired compound.

3-methyl-N-(1-phenylheptylidene)-2-pyridinamine (10):

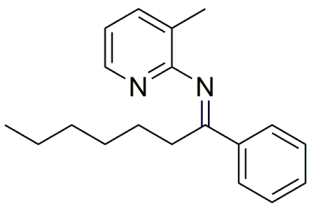

The reaction was carried out according to general procedure II with 9 (74 mg, 0.38 mmol, 1 eq.),

hex-1-ene (158 mg, 1.9 mmol, 5 eq.), dry K_2CO_3 (155 mg, 1.1 mmol, 3 eq.) and $[RhCl(PPh_3)_3]$ (35 mg, 0.038 mmol, 0.1 eq.) in dry and degassed toluene (3 ml). The reaction mixture was heated for 3 h at 150 °C. The general work-up procedure for C-H activation reactions was followed (PE/CH_2Cl_2/Et_3N 97:2:1). Yellowish oil (43 mg, 41% yield). ^{1}H-NMR (CD_2Cl_2, 200 MHz): δ = 0.79 (t, J = 7.1 Hz, 3 H), 1.02-1.32 (m, 6 H), 1.39-1.62 (m, 2 H), 2.13 (s, 3 H), 2.63 (m, 2 H), 6.96 (dd, J = 7.1, 5.0 Hz, 1 H), 7.37-7.58 (m, 4 H), 7.92-8.08 (m, 2H), 8.25 (d, J = 4.2 Hz, 1H) ppm. ^{13}C-NMR (CD_2Cl_2, 100 MHz): δ = 14.3, 17.7, 22.9, 27.96, 29.81, 31.58, 31.72, 119.45, 124.1, 128.3, 128.9, 131.1, 138.5, 138.9, 146.5, 162.6, 171.41 ppm. HRMS: calculated for $C_{19}H_{25}N_2$ $[M + H]^+$ 281.2012; found 281.2002. IR (ATR): $\tilde{\nu}_{C=N}$ = 1635 cm^{-1}.

2.16 Reaction on a bigger scale

The experiment was carried out according to general procedure I on a 0.5 mmol scale with a concentration of 0.25 mol/l of benzylamine **1** in the solvent and optimized reaction conditions for the direct alkylation of benzylic amines with alkenes were used. K_2CO_3 with a content of adsorbed water of 2 ± 1% was used.

The reaction was carried out according to general procedure I with **1** (100 mg, 0.5 mmol, 1 eq.), hex-1-ene (127 mg, 1.5 mmol, 3 eq.), K_2CO_3 (209 mg, 1.5 mmol, 3 eq.) and $[RhCl(cod)]_2$ (12 mg, 0.025 mmol, 0.05 eq.) in dry and degassed toluene (2 ml). The reaction mixture was heated for 3h at 150°C. The general work-up procedure for C-H activation reactions was followed (PE/EtOAc 99:1) and the products **4** (61%), **5** (8%) and **6** (9%) were isolated.

N-(1-phenylheptyl)-3-methylpyridin-2-amine (4):

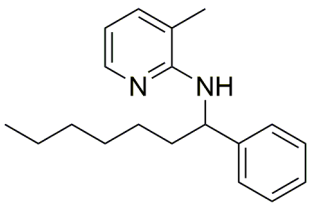

Colourless oil (87 mg, 61% yield). Although this compound was reported in literature[4] no analytical data was available. ^{1}H-NMR ($CDCl_3$, 200 MHz): δ = 0.85 (t, J = 6.9 Hz, 3 H), 1.11-1.50 (m, 8 H), 1.71-1.99 (m, 2 H), 2.10 (s, 3 H), 4.36 (d, J = 7.4 Hz, 1 H), 5.23 (q, J = 7.2 Hz, 1 H), 6.45 (dd, J = 7.0, 5.1 Hz, 1 H), 7.12-7.43 (m, 6 H), 7.95 (dd, J = 5.0, 1.5 Hz, 1H) ppm. ^{13}C-NMR ($CDCl_3$, 50 MHz): δ = 14.1, 17.1, 22.6, 26.3, 29.3, 31.8, 37.6, 54.7, 112.5, 116.2, 126.5, 126.7, 128.4, 136.8, 144.6, 145.5, 156.1 ppm. HRMS: calculated for $C_{19}H_{27}N_2$ $[M + H]^+$ 283.2169; found 283.2173.

N-Benzhydryl-3-methylpyridin-2-amine (5):

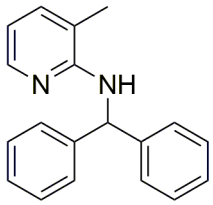

Colourless oil (8 mg, 6% yield). Analytical data was in accordance to literature reports.[1]

N-(tridecan-7-yl)-3-methylpyridin-2-amine (6):

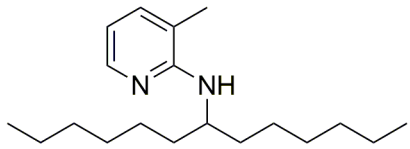

Colourless oil (12 mg, 9% yield). ^{1}H-NMR ($CDCl_3$, 200 MHz): δ = 0.86 (t, J = 6.8 Hz, 3 H), 1.11-1.70 (m, 20 H), 2.05 (s, 3 H), 3.82 (d, J = 8.0 Hz, 1 H), 4.22 (m, 1 H), 6.44 (dd, J = 7.0, 5.1 Hz, 1 H), 7.17 (d, J = 7.0 Hz, 1.0 Hz, 1 H), 7.98 (dd, J = 5.0, 1.5 Hz, 1H) ppm. ^{13}C-NMR ($CDCl_3$, 50 MHz): δ = 14.1, 17.1, 22.6, 25.7, 29.5, 31.9, 35.2, 50.1, 111.7, 115.9, 136.6, 145.4, 156.9 ppm. HRMS: calculated for $C_{19}H_{35}N_2$ $[M + H]^+$ 291.2795; found 291.2786.

3. Mathematical derivations, calculations and kinetic data

Errors given for regression parameters are standard errors and not standard deviations. Numbers are rounded to the last given digit. Errors given for derived parameters are determined using error propagation.

It should be noted that K_2CO_3 was more or less insoluble in the reaction mixture and the amounts used were far above its solubility limit. Therefore, concentration may not be the right term to denote its initial amount and maybe loading would be a more suitable term. However, it is more convenient to use the term concentration for all starting materials involved.

3.1 Kinetic profiles

Scheme S9.

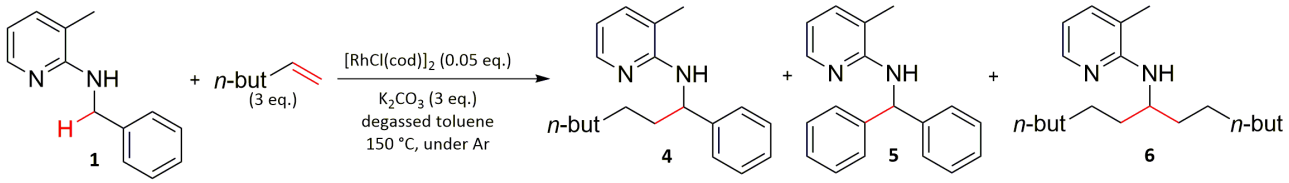

The data points for the kinetic time course of the direct C-H alkylation using hex-1-ene is shown in Table S2. The following table shows the initial concentrations of all the starting materials.

1	Hex-1-ene	K_2CO_3	$[RhCl(cod)]_2$
0.125 mol/l	0.375 mol/l	0.377 mol/l	0.00625 mol/l

Table S2: Data points for the kinetic time course of direct C-H alkylation of **1** using hex-1-ene. Percentages are calibrated GC-yields.

Time [h]	**1**	Error **1**	**6**	Error **6**	**4**	Error **4**	**5**	Error **5**
0.067	100%	2%	0.00%	0.00%	2.3%	0.4%	0.00%	0.00%
0.096	93%	2%	0.32%	0.09%	9.0%	0.4%	0.06%	0.03%
0.117	74%	4%	0.8%	0.3%	11%	1%	0.06%	0.02%

0.167	69%	3%	0.9%	0.3%	12%	1%	0.07%	0.04%
0.250	58%	6%	1.8%	0.5%	19%	2%	0.20%	0.08%
0.417	45%	5%	3.7%	0.3%	29%	4%	0.42%	0.03%
0.667	30%	2%	5.0%	0.1%	37.1%	0.4%	0.74%	0.07%
1.00	16%	3%	5.9%	0.3%	47%	3%	1.1%	0.1%
2.00	0.0%	0.0%	7.2%	0.5%	65%	6%	2.9%	0.5%
3.00	0.0%	0.0%	7.7%	0.3%	63%	3%	3.5%	0.1%
4.00	0.0%	0.0%	7.8%	0.7%	62%	3%	3.0%	0.6%
6.03	0.0%	0.0%	7.9%	0.7%	63%	1%	3.2%	0.6%

Since complete kinetic profiles were obtained for **1** and the products **4**, **5** and **6** mathematical functions were fitted to the data points. The function forms used for the regressions were derived from the exact solutions of simple kinetic models which are also shortly outlined. Regression parameters were determined by non-linear regression. In order to get more reliable regression parameters the time values were corrected for the time needed for the reaction mixture to reach a constant temperature which is given at the end of this section. This is necessary since kinetic profiles show the biggest changes in the beginning and without the correction the obtained regression parameters are significantly different.

The kinetic profile for the consumption of **1** was fitted to a simple exponential decomposition which is valid for unimolecular irreversible decomposition (Figure S1). The residual plot shows bigger residuals at the beginning and very small residuals at later reaction times. However, this is the case because the concentration of **1** approaches and also reaches 0. At the constant value of 0 the error cannot be high. The graph showing the data points together with the fitted function shows that the used mathematical function is only able to describe the kinetic profile of **1** roughly and not very accurate. However, a better plausible mathematical function with a reasonable number of parameters could not be found. We decided to make a reasonable compromise between number of parameters and accuracy of the resulting fit.

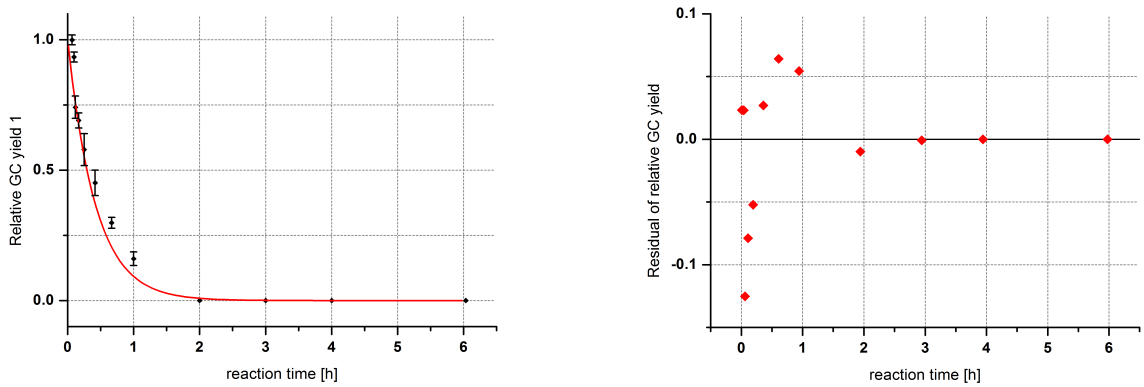

$$y = e^{-ax}$$

a		Statistics	
Value	Error	R^2	F
2.38	0.20	0.97883	1151.40

Figure S1: Regression result (left) and residual plot (right) for the consumption of **1**. The used regression equation and the regression result are shown in the lower section.

The kinetic profile for the formation of **4** was fitted to an equation which is valid for the formation of the product in a unimolecular reversible reaction (Figure S2). The residual plot reveals that the residuals are basically homoscedastic. In general the chosen mathematical function describes the kinetic behaviour of **4** in this reaction quite accurately.

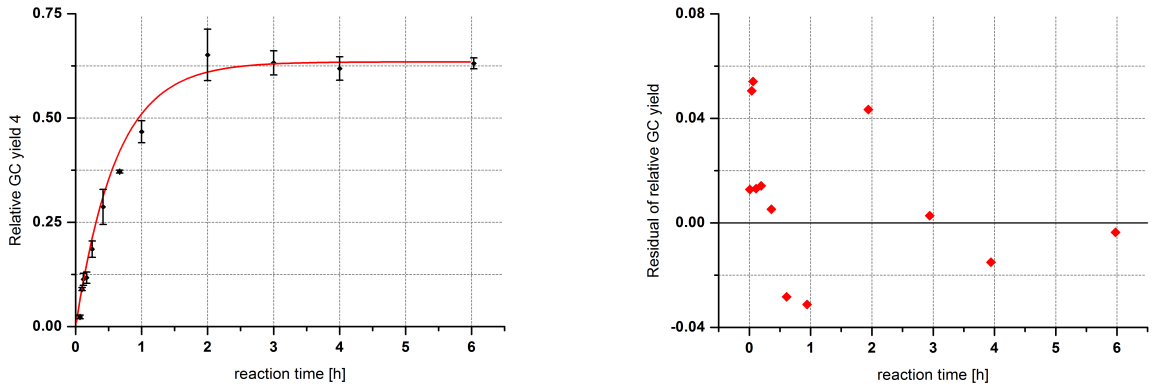

$$y = \frac{a}{a+b}\left[1 - e^{-(a+b)x}\right]$$

a		b		Statistics	
Value	Error	Value	Error	R^2	F
1.03	0.08	0.60	0.07	0.98472	1057.03

Figure S2: Regression result (left) and residual plot (right) for the formation of **4**. The used regression equation and the regression result are shown in the lower section.

The kinetic profile for the formation of **6** was fitted to the same equation as used for the formation of **4** (Figure S3). The residual plot reveals that the used function may not be suitable to describe the kinetic behaviour at the beginning. However, the deviation is not too big. The deviation comes from the presence of a short induction period for the formation of **6** since it is formed in a consecutive reaction from the initial product **4**.

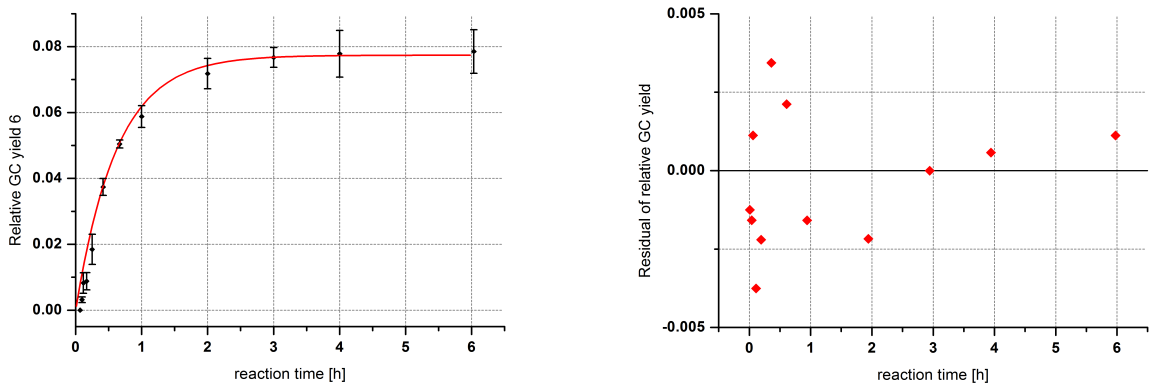

$$y = \frac{a}{a+b}\left[1 - e^{-(a+b)x}\right]$$

a		b		Statistics	
Value	Error	Value	Error	R^2	F
0.12	0.01	1.48	0.08	0.99556	3146.41

Figure S3: Regression result (left) and residual plot (right) for the formation of **6**. The used regression equation and the regression result are shown in the lower section.

The kinetic profile for the formation of **5** was tried to be fitted to an equation which describes the formation of C in the following kinetic scheme.

$$A \xrightarrow{k_1} B \underset{k_{-2}}{\overset{k_2}{\rightleftharpoons}} C$$

The corresponding mathematical function has the following form.

$$y = 1 - e^{-ax} - \frac{c}{b}\left[1 - e^{-bx}\right] - \frac{a-c}{b-c}\left[e^{-ax} - e^{-bx}\right]$$

However, since the resulting parameters yielded an insignificant result the mathematical form was slightly changed. The problem was that the resulting values for a, b and c were very similar, resulting in a difference very similar to zero with a significantly higher standard error. However, omitting the last term was sufficient to yield significantly better values. The residual plot shows slightly bigger residuals at later reaction times but the differences are not significant and the

standard deviations of those data points are also bigger.

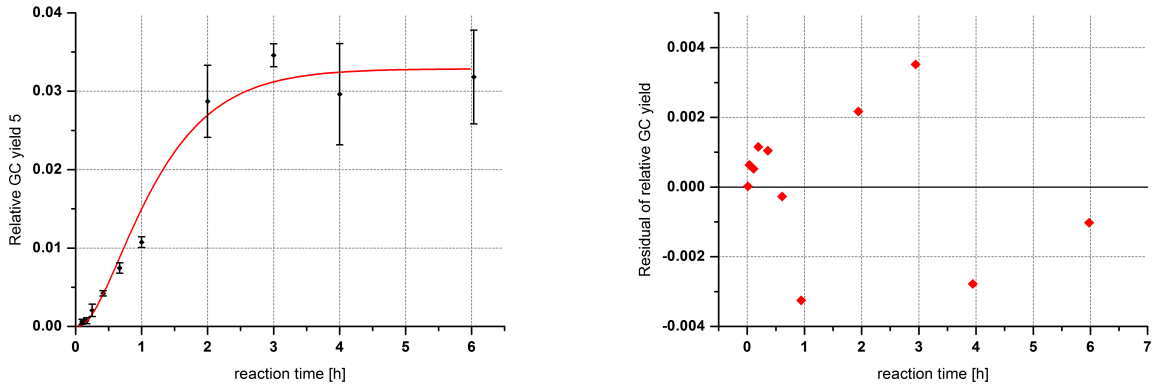

$$y = 1 - e^{-ax} - c[1 - e^{-bx}]$$

a		b		c		Statistics	
Value	Error	Value	Error	Value	Error	R^2	F
1.6	0.3	1.6	0.3	0.967	0.001	0.98184	305.01

Figure S4: Regression result (left) and residual plot (right) for the formation of **5**. The used regression equation and the regression result are shown in the lower section.

From the kinetic profile of the alkene reaction we also needed to extrapolate the data to determine the point at which the reaction starts formally. Therefore, we assume, as can also be seen by the data of the kinetic profiles and also from the experiments to determine the temperature dependence of the rate (vide infra), that the formation of product is a linear function of time in the initial reaction period (This assumption is reasonable since based on the data of the kinetic profiles and especially the experiments to determine the temperature dependence of the reaction rate no considerable induction period was observed). The reason this needs to be done is that the reaction mixture needs some time to reach a constant temperature. Experiments were conducted to determine how long it takes the reaction mixture to reach a constant temperature, and for reactions at 150 °C (temperature of the aluminium block) after 4 min the temperature remains more or less constant. However, even

after 3 min the reaction temperature does not change significantly thereafter. Therefore, it is reasonable that a line through the two data points at 4 min and at 5.75 min would result in a good estimate of the formal reaction starting point since between those data points the assumption of a linear increase in the product concentration is satisfied best. It should be noted that this in fact only influences the absolute initial rate values obtained and therefore rate constants derived from initial rate experiments. However, partial reaction orders and other relative magnitudes are not affected at all.

Effective reaction start in initial rate experiments: 3.4 min

From those two data points also the initial rate for the alkene reaction at those starting material concentrations is calculated. Since compound **6** is obviously formed from compound **4** the initial rate is calculated as sum of the initial rates for both compounds.

Initial rate: $(8.2 \pm 0.3) \cdot 10^{-5}$ mol $\cdot$ l^{-1} $\cdot$ s^{-1}

3.2 Initial rate experiments

First we must define the initial reaction period. Assuming the kinetic time profile for the formation of **4** would exactly follow the mathematical function determined by regression in the previous section, the relative error of the initial rate approximated by the method of initial rates at a product yield of 12% is only 10%, at a product yield of 18% the relative error is already 15% and at a product yield of 24% the relative error reaches a value of 20%. Therefore, in experiments using the method of initial rates the product yield should not reach values higher than 20% in order to keep the relative error in a reasonable range. So the method of initial rates is applied to a time period where the yield of the product is below 20%. only calculated for the cases that either both K_2CO_3 and $[RhCl(cod)]_2$ are below or above the respective borderline concentrations.

3.2.1 Initial rate dependence on the water content

The data points for the dependence of the initial rate on the content of adsorbed water in K_2CO_3 are given in Table S3.

Table S3: Data points for the dependence of the initial rate on the adsorbed water content in K_2CO_3.

Net c(K_2CO_3) [mol/l][1]	Adsorbed H_2O [m/m %]	Rate [10^{-5} mol · l^{-1} · s^{-1}]	Error of rate [10^{-5} mol · l^{-1} · s^{-1}]
0.371	0.000	0.77	0.06
0.371	0.018	7.0	0.4
0.360	0.152	8.5	0.5

1. Actual amount of K_2CO_3 accounting for the adsorbed water.

The initial rate shows a pronounced dependence on the adsorbed water content in K_2CO_3. Using freshly dried base the initial rate drops by one order of magnitude.

3.3 Kinetic isotope effect studies

3.3.1 Correction for H-D exchange during the reaction

In this section the method we used to correct the kinetic isotope (KIE) determined by the initial rates of a reaction with both unlabelled and isotopically labelled starting materials is derived.

First all the parameters used in the derivation are defined.

r_H .....Initial rate of the reaction with unlabelled (H) starting material $[\text{mol l}^{-1}\,\text{s}^{-1}]$

r_D .....Initial rate of the reaction with isotopically labelled (D) starting material $[\text{mol l}^{-1}\,\text{s}^{-1}]$

r_{obs} .....Observed initial rate with mixture isotopically labelled and unlabelled starting materials $[\text{mol l}^{-1}\,\text{s}^{-1}]$

x_H .....Mole fraction of unlabelled starting material in the reaction mixture

x_{Ha} .....Mole fraction of unlabelled starting material at the effective reaction start time

x_{He} .....Mole fraction of unlabelled starting material at the effective reaction end time

x_D .....Mole fraction of isotopically labelled starting material in the reaction mixture

t .....Reaction time $[s]$

t_a .....Effective start time of the reaction $[s]$

t_e .....Effective end time of the reaction $[s]$

c_{obs} .....Observed concentration of reaction product in the experiment $[mol\ l^{-1}]$

The general simplified approach is that the change of product concentration over time is a linear combination of product formed from unlabelled starting material and product formed from isotopically labelled starting material.

$$dc_{obs} = r_H x_H(t)dt + r_D x_D(t)dt \tag{1}$$

The following equation is assumed in order to eliminate one of the two mole fractions.

$$x_D(t) = 1 - x_H(t) \tag{2}$$

Equation 6 is substituted in equation 5.

$$dc_{obs} = (r_H - r_D)\, x_H(t)\, dt + r_D\, dt \tag{3}$$

Integration of equation7 yields the following assuming the reaction is in the initial reaction period and the reaction rates are independent from time in that reaction period.

$$c_{obs} = \int_{t_a}^{t_e} (r_H - r_D)\, x_H(t)\, dt + r_D\,(t_e - t_a) \tag{4}$$

$$r_{obs} = \frac{c_{obs}}{t_e - t_a} = r_D + \frac{r_H - r_D}{t_e - t_a} \int_{t_a}^{t_e} x_H(t)\, dt \tag{5}$$

This general formula allows determination of the true initial rate of the reaction with isotopically

labelled starting material from the observed initial rate if the time dependence of the mole fraction of unlabelled starting material over the course of the reaction is known.

In an optimum case this time dependence can be measured directly with an in-situ method. Integration can then be performed with usual approximative integration methods. However, when for any reason an in-situ method cannot be used either a lot of additional experiments have to be performed to determine the time dependence of this mole fraction accurately or this time dependence needs to be simplified in order to reduce the number of necessary experiments. The simplest case would be to determine this mole fraction at the effective start of the reaction and at the end of the reaction and assuming linear time dependence in between. Besides being very simple this method also has the advantage that it is more likely to underestimate the true initial rate of the reaction with isotopically labelled starting material rather than overestimate it because the time dependence of the mole fraction is more likely to have a negative curvature. So corrected KIE values are therefore estimated to be slightly lower by this method. Keeping this in mind is important to correctly interpret corrected KIE values.

In order to integrate equation 9 a linear dependence of x_H on time is assumed. For this linear dependence x_{Ha} and x_{He} at the time points t_a and t_e respectively are known and therefore its analytical form can easily be derived by solving a system of two linear equations. The corresponding solution is given in equation 10.

$$x_H(t) = \frac{x_{He} - x_{Ha}}{t_e - t_a}\, t + \frac{x_{Ha}\, t_e - x_{He}\, t_a}{t_e - t_a} \tag{6}$$

From equations 9 and 10 the integral can easily be determined and the equation can be solved for the initial rate of only the isotopically labelled starting material.

$$r_{obs} = r_D + \frac{r_H - r_D}{t_e - t_a}\left[\frac{x_{He} - x_{Ha}}{2(t_e - t_a)}\left(t_e^{\,2} - t_a^{\,2}\right) + \frac{x_{Ha}\, t_e - x_{He}\, t_a}{t_e - t_a}(t_e - t_a)\right] \tag{7}$$

$$r_{obs} = r_D + \frac{r_H - r_D}{t_e - t_a}\left[\frac{1}{2}\left(x_{He}\, t_e - x_{Ha}\, t_e + x_{He}\, t_a - x_{Ha}\, t_a\right) + x_{Ha}\, t_e - x_{He}\, t_a\right] \tag{8}$$

$$r_{obs} = r_D + \frac{r_H - r_D}{t_e - t_a}\left[\frac{x_{He} - x_{Ha}}{2(t_e - t_a)}\left(t_e^2 - t_a^2\right) + \frac{x_{Ha}\,t_e - x_{He}\,t_a}{t_e - t_a}(t_e - t_a)\right] \quad (7)$$

$$r_{obs} = r_D + \frac{r_H - r_D}{t_e - t_a}\frac{1}{2}\left(x_{He}\,t_e + x_{Ha}\,t_e - x_{He}\,t_a - x_{Ha}\,t_a\right) \quad (9)$$

$$r_{obs} = r_D + \frac{r_H - r_D}{2(t_e - t_a)}\left(x_{He} + x_{Ha}\right)\left(t_e - t_a\right) \quad (10)$$

$$r_{obs} = r_H\frac{\left(x_{He} + x_{Ha}\right)}{2} + r_D\left(1 - \frac{\left(x_{He} + x_{Ha}\right)}{2}\right) \quad (11)$$

$$r_D = \frac{r_{obs} - r_H\dfrac{\left(x_{He} + x_{Ha}\right)}{2}}{1 - \dfrac{\left(x_{He} + x_{Ha}\right)}{2}} \quad (12)$$

This equation allows for an easy correction of the observed initial rate in an experiment to determine the initial rate with isotopically labelled starting material in order to determine a KIE when there is also a high degree of H-D exchange going on during the reaction at a similar or even slightly higher rate.

3.3.2 Kinetic isotope effect results

KIE studies were conducted by determining the initial reaction rates for both using deuterated starting materials and undeuterated starting materials. KIE values were obtained from comparing the obtained initial rates.

Scheme S10.

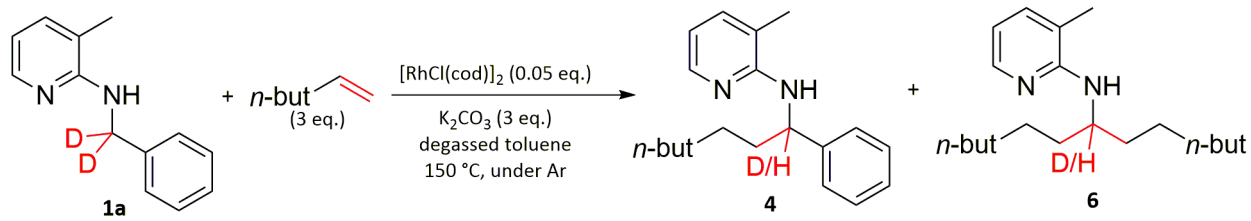

The data points for the determination of the KIE of the benzylic C-H bond are given in Table S4. The following table shows the initial concentrations of all the starting materials in these experiments except K_2CO_3. The KIE was first determined from uncorrected rates since the H-D

exchange was not very high. However, also corrected values are given for comparison.

1/**1a**	Hex-1-ene	$[RhCl(cod)]_2$
0.125 mol/l	0.375 mol/l	0.00625 mol/l

Table S4: Data points for the determination of the KIE of the benzylic C-H bond.

Compound	Adsorbed H_2O [m/m %]	$c_0(K_2CO_3)$ [mol/l]	Rate [10^{-5} mol · l^{-1} · s^{-1}]	Error of rate [10^{-5} mol · l^{-1} · s^{-1}]	H-content of **1** after reaction[1]	GC-yield of **4** + **6**
H	0.152	0.378	8.2	0.3	-	9.5%
D (>99%)	0.152	0.378	1.9	0.2	7%	1.9%
H	0.018	0.378	7.0	0.4	-	8.2%
D (>99%)	0.018	0.379	1.5	0.2	5%	1.5%

1. Determined by ^{1}H-NMR analysis of the crude reaction mixture after filtration and removal of the solvent under reduced pressure.

From these data points the KIE value of the benzylic C-H bond using K_2CO_3 with an adsorbed water content of about 15% was determined to be 4.3 ± 0.6 indicating a significantly slower reaction using the corresponding deuterated compound. Correcting this KIE for the H-D exchange during the reaction assuming full deuteration before the start of the reaction a value of 4.9 ± 0.8 is obtained. Using K_2CO_3 with an adsorbed water content of only about 2% the KIE was 4.7 ± 0.6 so basically the same showing that the KIE of the benzylic C-H bond is independent of the adsorbed water content of K_2CO_3. The corrected KIE would be 5.2 ± 0.8 so even more alike. Both values are indicative of a primary KIE. Another thing to notice is the deuterium content in the remaining starting material after the reaction. The H-D exchanges were actually higher than the sum of the yields of the products in the experiments using the deuterated starting material **1a**. This is actually quite surprising and will be explained later.

Scheme S11.

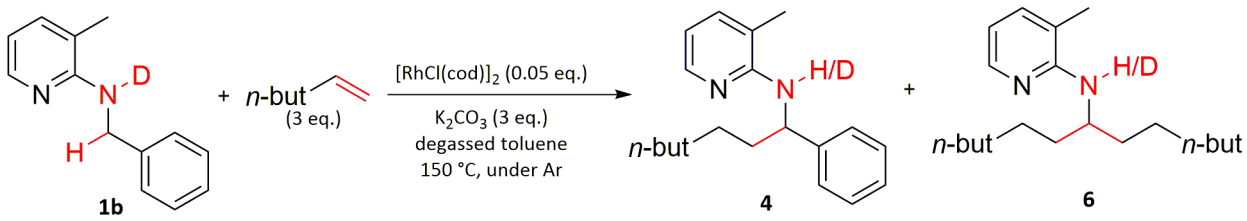

The data points for the determination of the KIE of the N-H bond are given in Table S5. The following table shows the initial concentrations of all the starting materials in these experiments except K_2CO_3.

1/**1b**	Hex-1-ene	$[RhCl(cod)]_2$
0.125 mol/l	0.375 mol/l	0.00625 mol/l

Table S5: Data points for the determination of the KIE of the N-H bond. Rates given in this table are uncorrected for the H-D exchange that occurred during the reaction.

Compound	Adsorbed H_2O [m/m %]	$c_0(K_2CO_3)$ [mol/l]	Rate [10^{-5} mol · l^{-1} · s^{-1}]	Error of rate [10^{-5} mol · l^{-1} · s^{-1}]	H-content of **1** after reation[1]
H	0.018	0.378	7.0	0.4	-
D (>95%)	0.018	0.378	6.3	0.8	(56 ± 1) %

1. Determined by IR analysis of the reaction mixture after filtration.

Before the results are calculated there is one major thing to notice. The KIE of the N-H bond could not be determined using K_2CO_3 with an adsorbed water content of about 15% since the N-D exchanged with the water from the base and before any product was formed the deuterium content in the starting material was only about 15%. Therefore correcting the obtained initial rate would have resulted in too large error margins. Using K_2CO_3 with an adsorbed water content of about 2% resulted in deuterium content after the reaction which was still quite high and allowed a reliable determination of the KIE of the N-H bond. In addition the deuterium content before the reaction

started and after stopping the reaction did not show significantly different values in these experiments so the deuterium content was assumed to be constant during the reaction at the value determined after stopping the reaction.

Moreover, since the H-content of **1** was determined by IR analysis from the corresponding N-H and N-D stretching vibration bands the value could show a deviation due to a different H-content in the product of the reaction because the corresponding bands overlap. However, since in these experiments only about 5% of products were formed the expected deviations in the H-content of **1** in a worst case scenario assuming only N-H being present in the product is only slightly outside the error margin (difference of 1.6 times the standard deviation to the determined value). In addition, the H-content in the product formed is expected to be similar to the H-content of the remaining starting material making this error effectively negligible.

From these data points the corrected KIE value of the N-H bond using K_2CO_3 with an adsorbed water content of about 2% was determined to be 1.3 ± 0.1. So maybe there is a small secondary KIE observed but a primary KIE can be excluded.

3.4 Investigation of imine intermediate kinetics

In order to determine whether the reaction mechanism proceeds over the corresponding imine or not it was necessary to distinguish between the three general scenarios which are outlined in the paper (Scheme 8 in the paper).

For the following mathematical derivation several variables are used.

a … Relative concentration of A (starting material)

i … Relative concentration of I (intermediate)

p … Relative concentration of P (product)

t … Time

k_1 … First-order rate constant for the reaction of A to I

k_2 … First-order rate constant for the forward reaction of I to P

k_{-2} … First-order rate constant for the backward reaction of P to I

It should be noted that all the rate constants are positive and for all the other variables values are bigger than or equal to 0.

Based on these mechanistic scenarios a method was developed to distinguish between them from kinetic data. First the following simplified kinetic model is assumed.

$$\mathbf{A} \xrightarrow{k_1} \mathbf{I} \underset{k_{-2}}{\overset{k_2}{\rightleftharpoons}} \mathbf{P}$$

Based on this simplified kinetic model the following system of differential equations can be formulated.

$$\frac{da}{dt} = -k_1 a \tag{13}$$

$$\frac{di}{dt} = k_1 a + k_{-2} p - k_2 i \tag{14}$$

$$\frac{dp}{dt} = -k_{-2} p + k_2 i \tag{15}$$

In addition, we assume that the sum of the concentrations of A, I and P equals 1.

$$a + i + p = 1 \tag{16}$$

The solution of this system of differential equations is straightforward and will not be discussed in detail. The initial conditions were that at time 0 the relative concentration of A is 1 and those of I and P are 0.

$$a(0) = 1 \tag{17}$$

$$i(0)=0 \tag{18}$$

$$p(0)=0 \tag{19}$$

The following solutions for the time-dependent relative concentrations of A, I and P are obtained in case that k_1 does not equal the sum of k_{-2} and k_2.

$$a(t)=e^{-k_1 t} \tag{20}$$

$$i(t)=\frac{k_{-2}}{k_{-2}+k_2}\left(1-e^{-(k_{-2}+k_2)t}\right)+\frac{k_1-k_{-2}}{k_{-2}+k_2-k_1}\left(e^{-k_1 t}-e^{-(k_{-2}+k_2)t}\right) \tag{21}$$

$$p(t)=1-e^{-k_1 t}-\frac{k_{-2}}{k_{-2}+k_2}\left(1-e^{-(k_{-2}+k_2)t}\right)-\frac{k_1-k_{-2}}{k_{-2}+k_2-k_1}\left(e^{-k_1 t}-e^{-(k_{-2}+k_2)t}\right) \tag{22}$$

As the difference of the sum of k_{-2} and k_2 and k_1 appears in the denominator in the functions for the relative concentrations of I and P this term is assumed to be unequal to 0 (which of course has to be assumed already during the derivation). In the case this equals 0 different solutions for the time course of the relative concentrations of I and P are obtained.

$$i(t)=\frac{k_{-2}}{k_{-2}+k_2}\left(1-e^{-(k_{-2}+k_2)t}\right)+\left(k_1-k_{-2}\right)t\,e^{-(k_{-2}+k_2)t} \tag{23}$$

$$p(t)=1-e^{-k_1 t}-\frac{k_{-2}}{k_{-2}+k_2}\left(1-e^{-(k_{-2}+k_2)t}\right)-\left(k_1-k_{-2}\right)t\,e^{-(k_{-2}+k_2)t} \tag{24}$$

To have a first idea of how these functions look like two plots were created. The values assigned to the rate constants are also given.

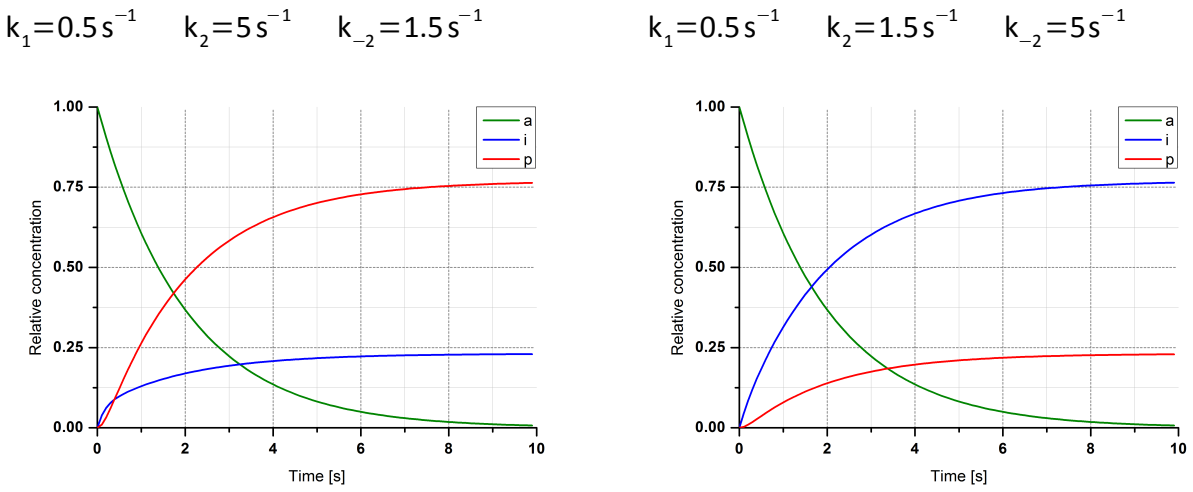

Figure S5: Diagrams showing the time profiles of A, I and P in the simplified kinetic model with two distinct sets of rate constants. In the left diagram P is the major product, in the right diagram I is the major product.

It can be seen that depending on the values of k_2 and k_{-2} either I or P is the major product in this model. Our method to distinguish between the three mechanistic scenarios is now based on the following feature. In an initial reaction period the intermediate I appears before the final product P does. This itself may already help to distinguish between the possible scenarios. However, in order to have a more general and reliable method instead of looking at the time profiles of I and P themselves the ratio of those should be calculated and plotted. This is done for the example plots.

$k_1 = 0.5\,s^{-1}$ $k_2 = 5\,s^{-1}$ $k_{-2} = 1.5\,s^{-1}$ $k_1 = 0.5\,s^{-1}$ $k_2 = 1.5\,s^{-1}$ $k_{-2} = 5\,s^{-1}$

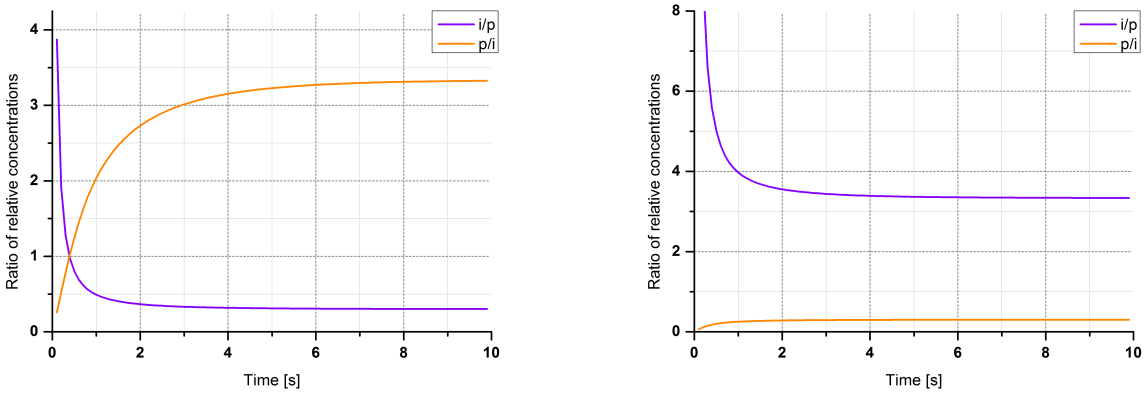

Figure S6: Diagrams showing the time course of both the ratio of I to P and P to I for the two special cases with the specified values for the rate constants given above.

It can clearly be seen that the general trend of those two function is the same in both cases. Trying several values for the rate constants did not result in a change to the general trend. The function representing the ratio of I to P seems to be strictly decreasing for positive time and the function representing the inverse therefore is strictly increasing. The mathematical proof for the monotonicity of these functions is outlined below. The monotonicity only needs to be proven for one of the two since the monotonicity of its inverse directly follows from the initial function.

In order to simplify these functions slightly for the following calculations a derived parameter is defined as follows.

$$k_2' = k_{-2} + k_2 \tag{25}$$

The functions for the relative concentrations of I and P change slightly to the following.

$$i(t) = \frac{k_{-2}}{k_2'}\left(1 - e^{-k_2' t}\right) + \frac{k_1 - k_{-2}}{k_2' - k_1}\left(e^{-k_1 t} - e^{-k_2' t}\right) \tag{26}$$

$$p(t)=1-e^{-k_1 t}-\frac{k_{-2}}{k_2'}(1-e^{-k_2' t})-\frac{k_1-k_{-2}}{k_2'-k_1}(e^{-k_1 t}-e^{-k_2' t}) \tag{27}$$

Now the function r(t) is defined as the ratio of P to I.

$$r(t)=\frac{p(t)}{i(t)}=\frac{1-e^{-k_1 t}-i(t)}{i(t)} \tag{28}$$

This function can now be slightly rearranged.

$$r(t)=\frac{1-e^{-k_1 t}-i(t)}{i(t)}=\frac{1-e^{-k_1 t}}{i(t)}-1 \tag{29}$$

Keeping in mind that the numerator equals the sum of I and P this can be rearranged further.

$$r(t)=\frac{1-e^{-k_1 t}}{i(t)}-1=\frac{i(t)+p(t)}{i(t)}-1 \tag{30}$$

From this equation it can now clearly be seen that r will be strictly increasing if this fraction is strictly increasing. The numerator is strictly increasing which can directly be seen when its first derivative with respect to the time is determined. Now there are two possibilities. If i(t) is decreasing it can trivially be seen that r(t) is increasing. If i(t) is increasing r(t) is only increasing if the numerator is increasing to a higher degree than the denominator. This is the case if p(t) is strictly increasing. Now p(t) is strictly increasing if its first derivative is always positive. This needs to be shown. We therefore determine the first derivative of p(t).

$$p'(t)=k_1 e^{-k_1 t}-k_{-2} e^{-k_2' t}-\frac{k_1-k_{-2}}{k_2'-k_1}(-k_1 e^{-k_1 t}+k_2' e^{-k_2' t}) \tag{31}$$

$$p'(t)=\frac{k_1 k_2'-k_1^2}{k_2'-k_1}e^{-k_1 t}-\frac{k_{-2}k_2'-k_{-2}k_1}{k_2'-k_1}e^{-k_2' t}+\frac{k_1^2-k_1 k_{-2}}{k_2'-k_1}e^{-k_1 t}-\frac{k_1 k_2'-k_{-2}k_2'}{k_2'-k_1}e^{-k_2' t} \tag{32}$$

$$p'(t)=\frac{k_1(k_2'-k_{-2})}{k_2'-k_1}\left(e^{-k_1 t}-e^{-k_2' t}\right) \tag{33}$$

The numerator of this term is always positive. Therefore two possibilities remain. The denominator can be positive or negative.

$$k_2'-k_1>0 \Leftrightarrow k_2'>k_1 \Leftrightarrow -k_2' t<-k_1 t \Leftrightarrow e^{-k_2' t}<e^{-k_1 t} \Leftrightarrow e^{-k_1 t}-e^{-k_2' t}>0 \tag{34}$$

This clearly shows that if the denominator is positive the whole term is positive for positive time and p(t) is strictly increasing. If the denominator is negative then also the difference of the two exponential functions is negative which can be seen by simply reversing all the inequations above and therefore p(t) is also strictly increasing. Now there is only the case remaining that the denominator equals 0 where the other equation for p(t) has to be taken (equation 24). In this case the following is valid.

$$k_2+k_{-2}=k_1 \tag{35}$$

The first derivative is calculated as follows starting with a simplification of the function p(t) which results from combining equations 24 and 35.

$$p(t)=1-e^{-k_1 t}-\frac{k_{-2}}{k_1}(1-e^{-k_1 t})-(k_1-k_{-2})te^{-k_1 t} \tag{36}$$

$$p'(t)=k_1 e^{-k_1 t}-k_{-2}e^{-k_1 t}-(k_1-k_{-2})e^{-k_1 t}+k_1(k_1-k_{-2})te^{-k_1 t} \tag{37}$$

$$p'(t)=k_1(k_1-k_{-2})te^{-k_1 t} \tag{38}$$

For positive time this term is always positive since k_1 is bigger than k_{-2}. Altogether it is shown that the function r(t) representing the ratio of P to I is strictly increasing for positive time. Assuming that the function r(t) does not vanish which is true for positive time it directly follows that the inverse function is strictly decreasing.

Overall, this provides us a method to distinguish between the first two mechanistic scenarios. It should be noted that so far we have not accounted for the third mechanistic scenario where the first two pathways occur at a similar rate. This will be done mathematically considering an extended kinetic model. Therefore we need one additional rate constant and for convenience the variables are named differently.

a … Relative concentration of A (starting material)

b … Relative concentration of B (product 1)

c … Relative concentration of C (product 2)

t … Time

k_1 … First-order rate constant for the reaction of A to B

k_1' … First-order rate constant for the reaction of A to C

k_2 … First-order rate constant for the forward reaction of B to C

k_{-2} … First-order rate constant for the backward reaction of C to B

Now we consider the following extended kinetic model.

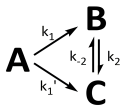

Based on this kinetic model the following system of differential equations can be formulated.

$$\frac{da}{dt} = -(k_1 + k_1')a \tag{39}$$

$$\frac{db}{dt} = k_1 a + k_{-2} c - k_2 b \tag{40}$$

$$\frac{dp}{dt} = -k_{-2} p + k_2 i \tag{41}$$

In addition, we also assume that the sum of the concentrations of A, B and C equals 1.

$$a+b+c=1 \tag{42}$$

The solution of this system of differential equations is straightforward as was the first one and will not be discussed in detail. The initial conditions were that at time 0 the relative concentration of A is 1 and those of B and C are 0.

$$a(0)=1 \tag{43}$$
$$b(0)=0 \tag{44}$$
$$c(0)=0 \tag{45}$$

The following solutions for the time-dependent relative concentrations of A, B and C are obtained for the case that the sum of k_1 and k_1' does not equal the sum of k_{-2} and k_2.

$$a(t)=e^{-(k_1+k_1')t} \tag{46}$$
$$b(t)=\frac{k_{-2}}{k_{-2}+k_2}+\frac{k_1-k_{-2}}{k_{-2}+k_2-k_1-k_1'}e^{-(k_1+k_1')t}+\left(\frac{k_{-2}-k_1}{k_{-2}+k_2-k_1-k_1'}-\frac{k_{-2}}{k_{-2}+k_2}\right)e^{-(k_{-2}+k_2)t} \tag{47}$$
$$c(t)=\frac{k_2}{k_{-2}+k_2}+\frac{k_1'-k_2}{k_{-2}+k_2-k_1-k_1'}e^{-(k_1+k_1')t}-\left(\frac{k_{-2}-k_1}{k_{-2}+k_2-k_1-k_1'}-\frac{k_{-2}}{k_{-2}+k_2}\right)e^{-(k_{-2}+k_2)t} \tag{48}$$

As the difference of the sum of k_{-2} and k_2 and the sum of k_1 and k_1' appears in the denominator in the functions for the relative concentrations of B and C this term is assumed to be unequal to 0 (which of course has to be assumed during the derivation). In the case this equals 0 different solutions for the time course of the relative concentrations of B and C are obtained.

$$b(t)=\frac{k_{-2}}{k_{-2}+k_2}\left(1-e^{-(k_{-2}+k_2)t}\right)+(k_1-k_{-2})te^{-(k_{-2}+k_2)t} \tag{49}$$
$$c(t)=\frac{k_2}{k_{-2}+k_2}\left(1-e^{-(k_{-2}+k_2)t}\right)-(k_1-k_{-2})te^{-(k_{-2}+k_2)t} \tag{50}$$

To have an idea of how these functions look like two plots were created. The values assigned to the rate constants are also given. Since considering a mechanistic scenario makes only sense if both reactions occur at a similar rate, similar values for k_1 and k_1' are taken in the examples.

$k_1 = 0.25\,s^{-1}$ $k_1' = 0.3\,s^{-1}$ $k_2 = 5\,s^{-1}$ $k_{-2} = 20\,s^{-1}$

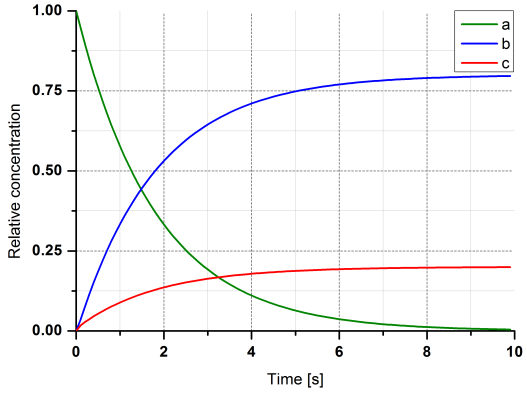

$k_1 = 0.25\,s^{-1}$ $k_1' = 0.3\,s^{-1}$ $k_2 = 30\,s^{-1}$ $k_{-2} = 35\,s^{-1}$

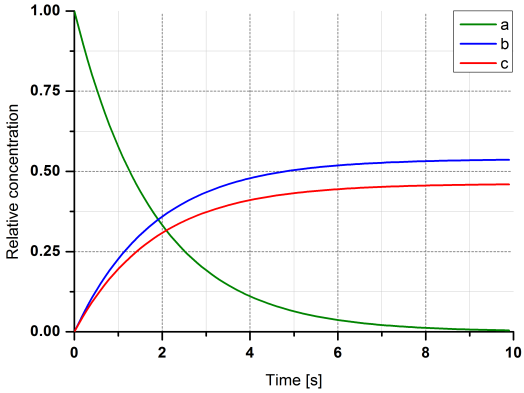

Figure S7: Diagrams showing the time profiles of A, B and C in the extended kinetic model with two distinct sets of rate constants. In the left diagram there is one major product in the right diagram two products are formed in similar amounts.

We again also look at the ratios of B and C and the inverse.

$k_1 = 0.25\,s^{-1}$ $k_1' = 0.3\,s^{-1}$ $k_2 = 5\,s^{-1}$ $k_{-2} = 20\,s^{-1}$

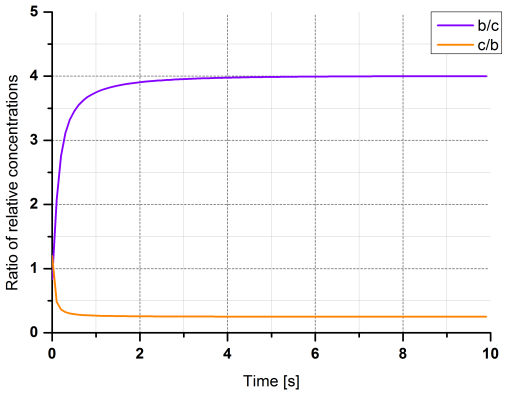

$k_1 = 0.25\,s^{-1}$ $k_1' = 0.3\,s^{-1}$ $k_2 = 30\,s^{-1}$ $k_{-2} = 35\,s^{-1}$

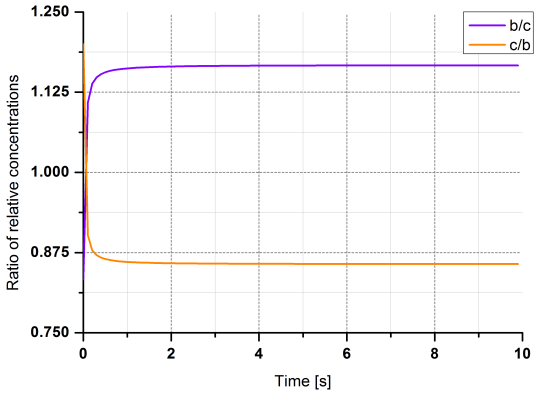

Figure S8: Diagrams showing the time course of both the ratio of B to C and C to B for the two special cases with the specified values for the rate constants given above.

From these two examples it can already be seen that the general trend of the two ratios will be comparable to the general trend of the ratios I to P or P to I for the simplified kinetic model we first discussed. We will not make a full curve discussion for the extended kinetic model but in general the ratios can show a very similar time course compared to the simplified kinetic model. The main differences are at the beginning. Assuming that both pathways occur the slopes of the concentration curves of products B and C are both finite at time 0 whereas the concentration curve of product P in the other kinetic model has a slope of 0. This has also a consequence to the ratio curves. For the extended kinetic model both curves have a finite value at time 0 whereas in the kinetic model allowing only one pathway the ratio of intermediate to product is converging infinity when time converges 0 and the ratio of product to intermediate is converging 0 when time converges 0.

The problem with these differences in curve forms is that they are observed at time 0 which is experimentally not accessible. Even if it can be approximated to an infinitely small difference limits of detection and quantification of the corresponding products will limit the determination of their

concentrations. Extrapolation from sufficiently near time points will not be reliable since the corresponding ratio curves have very high slopes in that time period. That are the reasons it is in principle impossible to distinguish those two mechanistic scenarios experimentally by this method.

This already shows the limits of our developed method. By looking at the time course of the product ratios it allows us to easily distinguish between the first two mechanistic scenarios. However, an overlap of both mechanistic scenarios (i.e. mechanistic scenario 3) cannot be excluded by this method. Similar methods to investigate reaction mechanisms are readily employed in the determination of biochemical reaction mechanisms.[5]

Now with the mathematical foundations of this method at hand we have a means to exclude one of the three mechanistic scenarios given in the beginning of that section by looking at the time course of the ratio of the alkylated imine **10** to the main reaction product **4**. From our previous experiments we looked at the area ratios of those compounds from GC chromatograms because besides a constant factor the area ratio corresponds to the ratio of the concentrations. The corresponding results are given in the following tables and figures.

Table S6: Data points for the GC area ratios of alkylated imine **10** and amine **4** at 150 °C obtained from the experiment series to determine the kinetic time course of the reaction.

Time [min]	GC Area Ratio **10**/**4**
4	0.043 ± 0.004
7	0.016 ± 0.004
10	0.013 ± 0.004
15	0.009 ± 0.002
25	0.005 ± 0.002
40	0.0047 ± 0.0009
60	0.0054 ± 0.0006
120	0.006 ± 0.001
180	0.0052 ± 0.0009
240	0.0063 ± 0.0008
362	0.0056 ± 0.0008

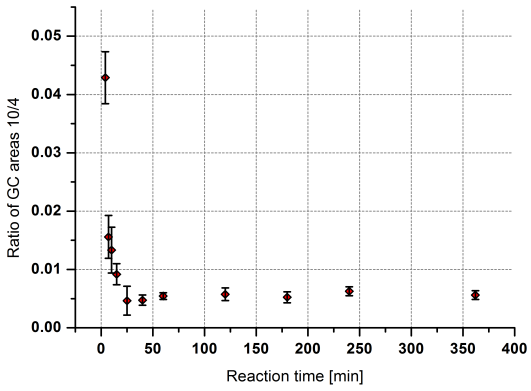

Figure S9: Ratio of GC areas of **10** to **4** obtained from the kinetic time profile.

In Figure S9 the ratio of alkylated imine **10** to the main reaction product **4** is decreasing over time andthe ratio reaches a constant value after the decreasing period. Based on the method we developed this excludes mechanistic scenario 1 where the alkylation reaction occurs only on the amine and the corresponding imines are only formed in off-cycle reactions. On the basis of this result the reaction mechanism actually proceeds over the corresponding imines. However, as outlined above mechanistic scenario 3 where the alkylation reaction takes place both at the amine and the imine at a similar rate cannot be excluded.

References

(1) Dastbaravardeh, N.; Kirchner, K.; Schnürch, M.; Mihovilovic, M. D. *J. Org. Chem.* **2013**, *78*, 658-672.

(2) Marce, P.; Godard, C.; Feliz, M.; Yanez, X.; Bo, C.; Castillon, S. *Organometallics* **2009**, *28*, 2976-2985.

(3) Jun, C.-H.; Lee, D.-Y.; Lee, H.; Hong, J.-B. *Angew. Chem. Int. Ed.* **2000**, *39*, 3070-3072.

(4) Jun, C.-H.; Hwang. D.-C.; Na, S.-J. *Chem. Commun.* **1998**, 1405-1406.

(5) Crampin, E. J.; Schnell, S.; McSharry, P. E. *Prog. Biophys. Mol. Biol.* **2004**, *86*, 77-112

4. NMR spectra of new compounds

NMR spectra of all new compounds are provided in the following pages.

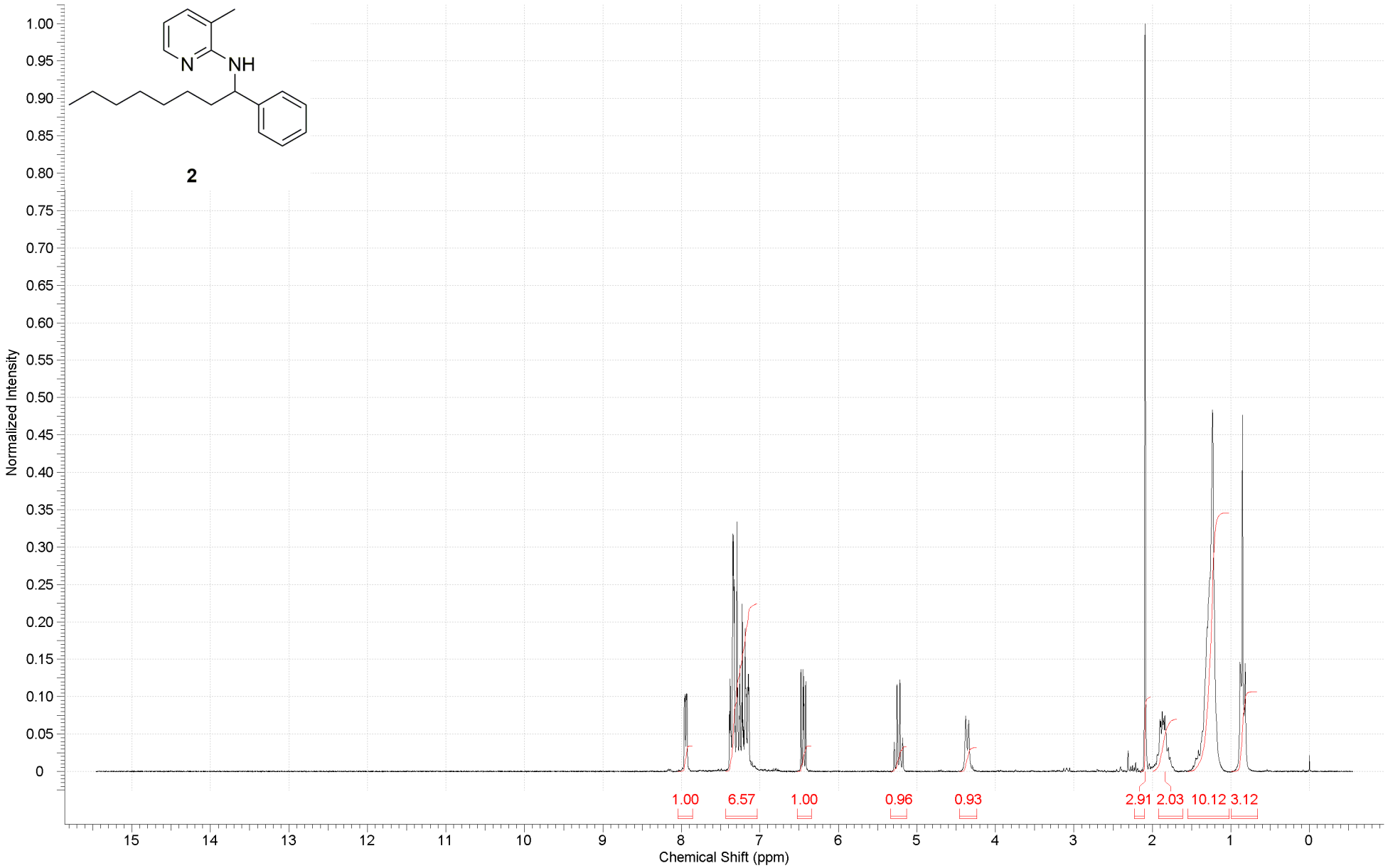
N
NH
2
Normalized Intensity
Chemical Shift (ppm)
1.00
6.57
1.00
0.96
0.93
2.91
2.03
10.12
3.12

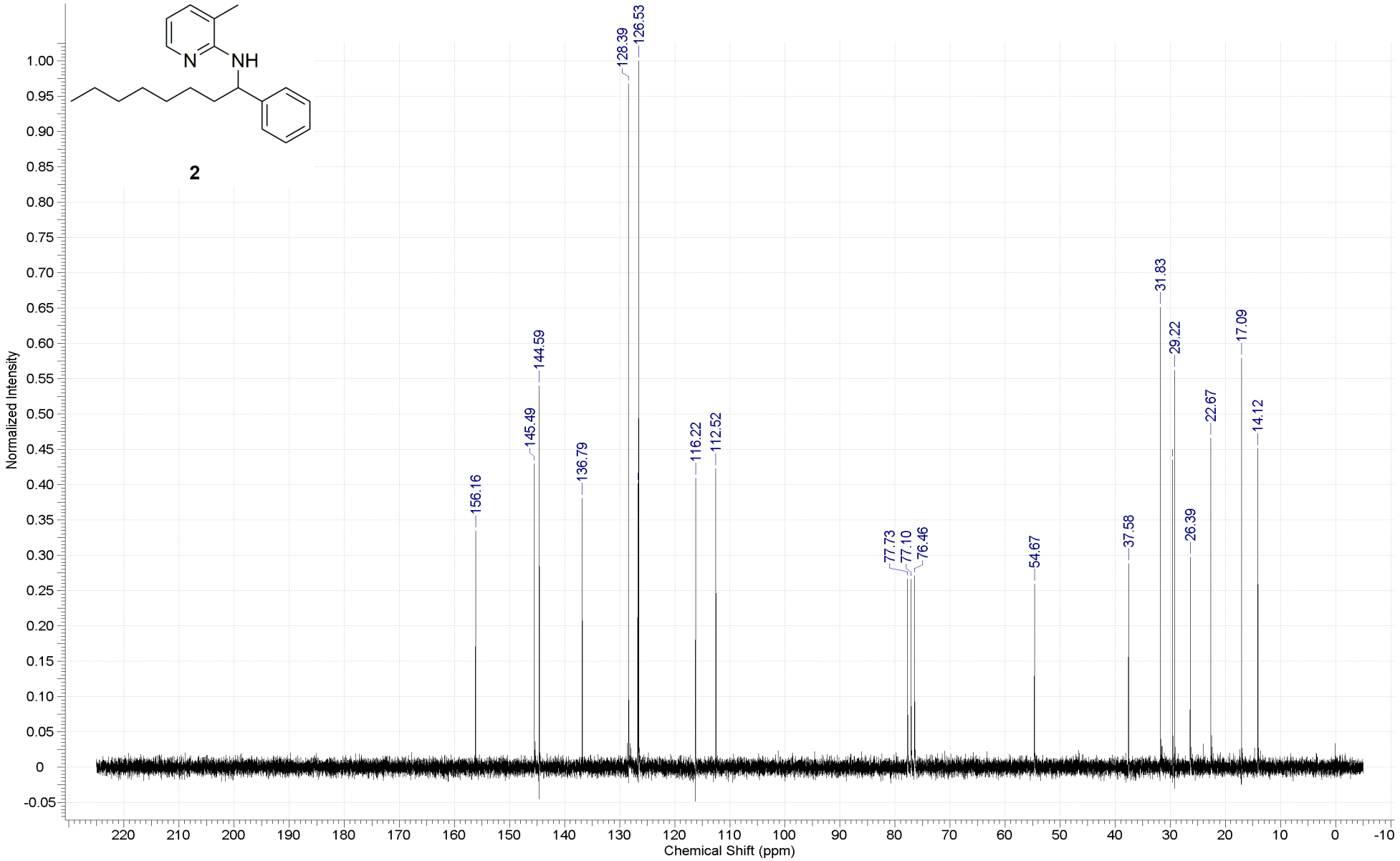
N
NH
2
Normalized Intensity
Chemical Shift (ppm)
156.16
145.49
144.59
136.79
128.39
126.53
116.22
112.52
77.73
77.10
76.46
54.67
37.58
31.83
29.22
26.39
22.67
17.09
14.12

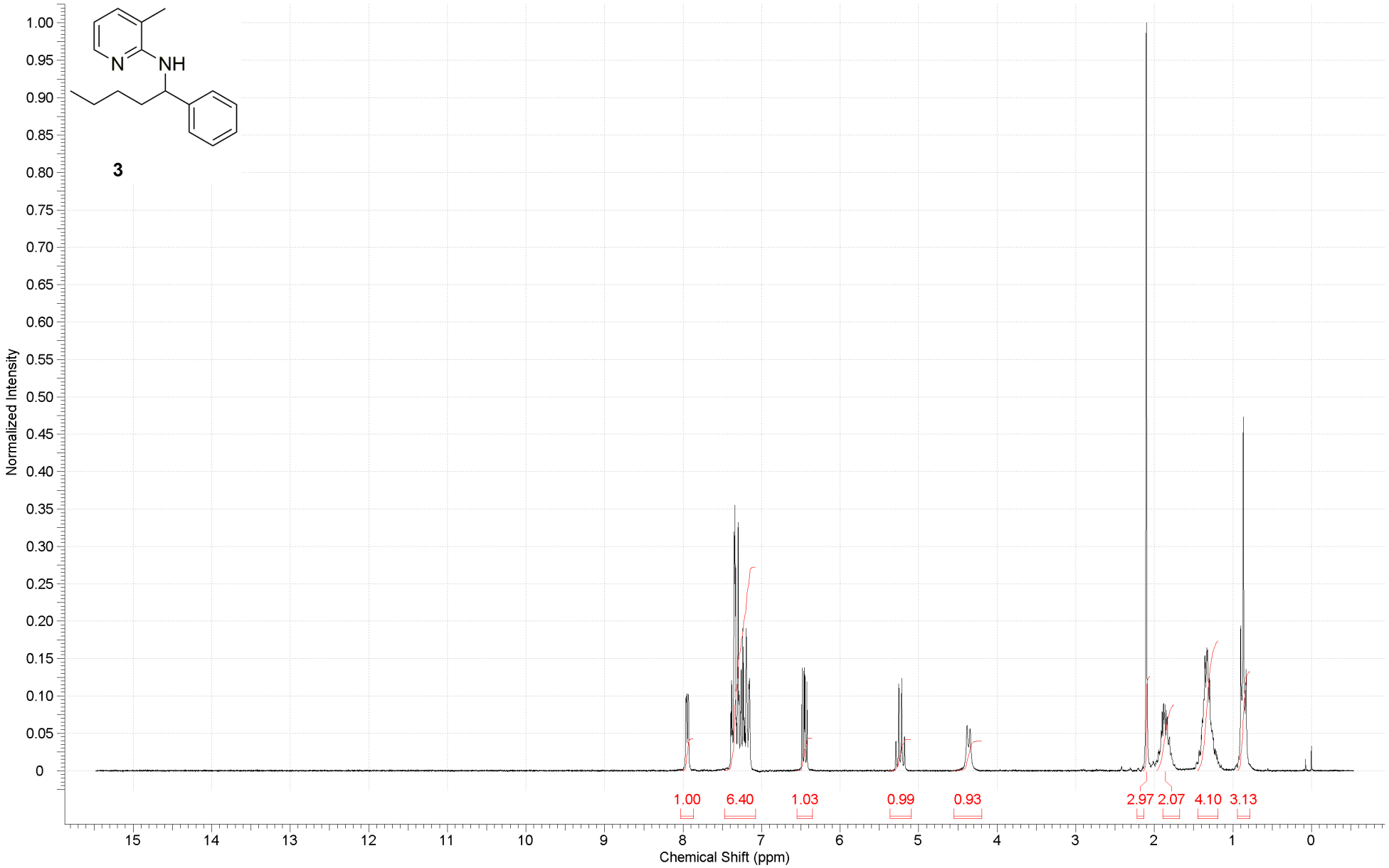
N
NH
3
Normalized Intensity
Chemical Shift (ppm)
1.00
6.40
1.03
0.99
0.93
2.97
2.07
4.10
3.13

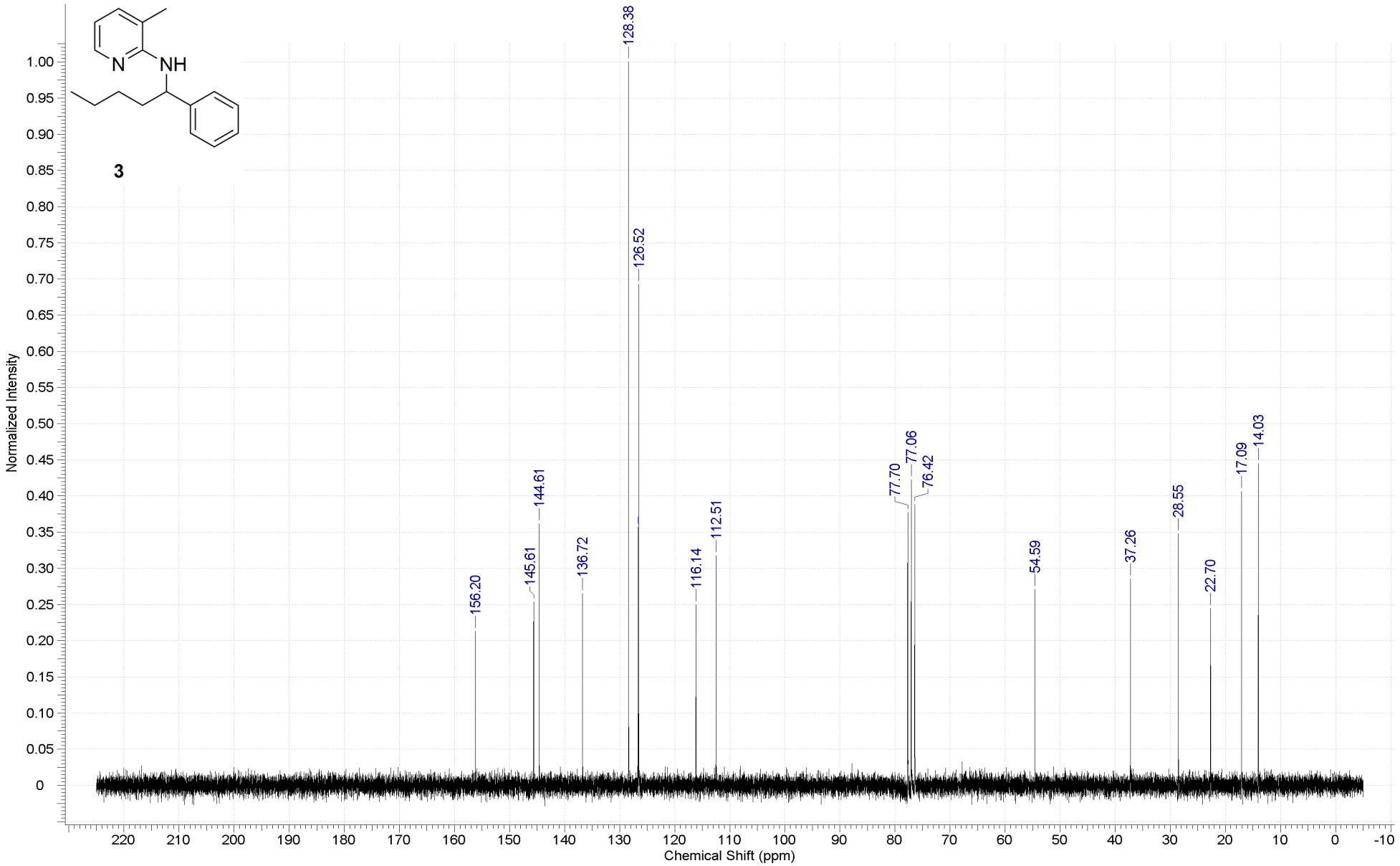
N
NH
3
128.38
126.52
156.20
145.61
144.61
136.72
116.14
112.51
77.70
77.06
76.42
54.59
37.26
28.55
22.70
17.09
14.03
Normalized Intensity
Chemical Shift (ppm)

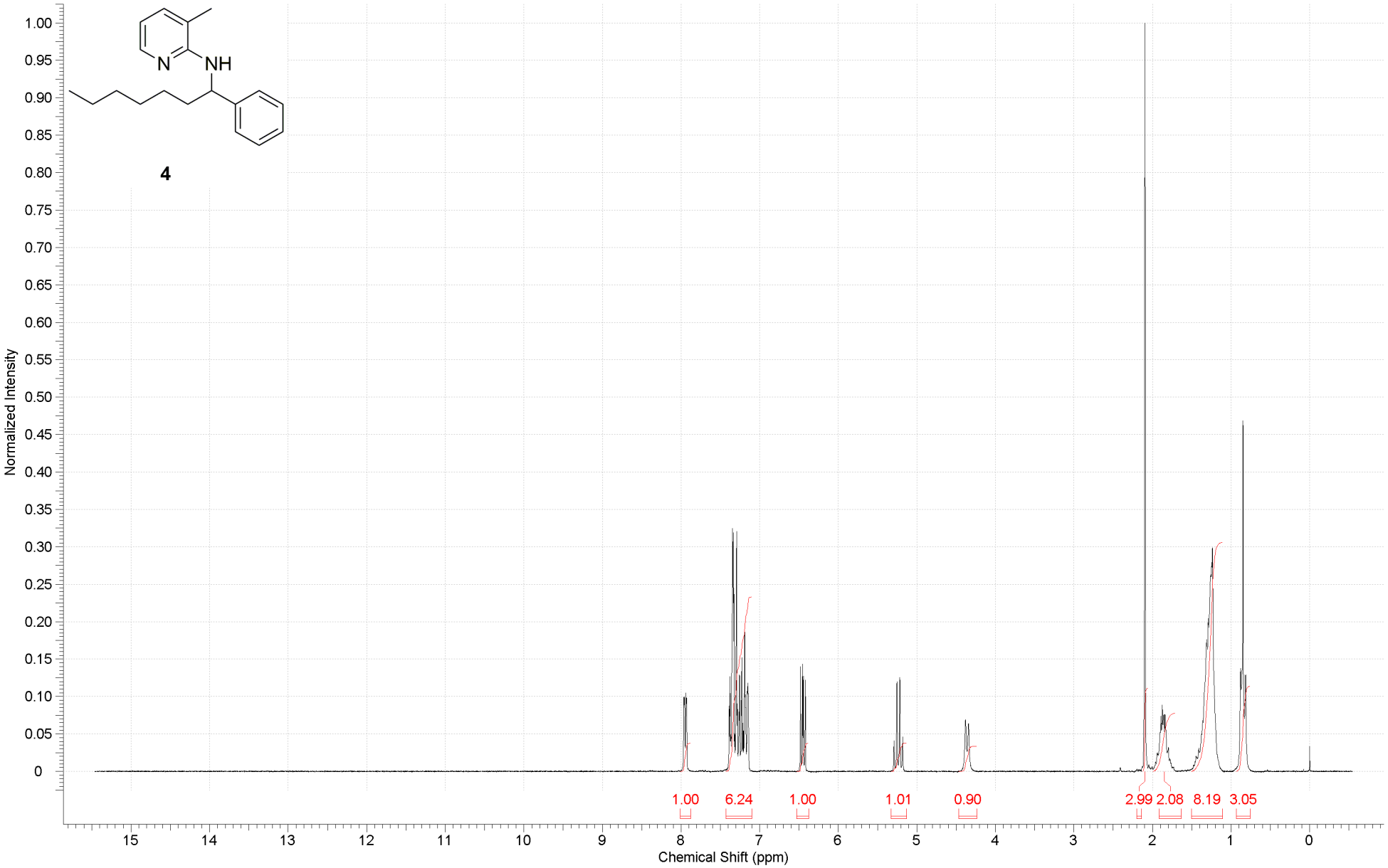
N
NH
4
Normalized Intensity
Chemical Shift (ppm)
1.00
6.24
1.00
1.01
0.90
2.99
2.08
8.19
3.05

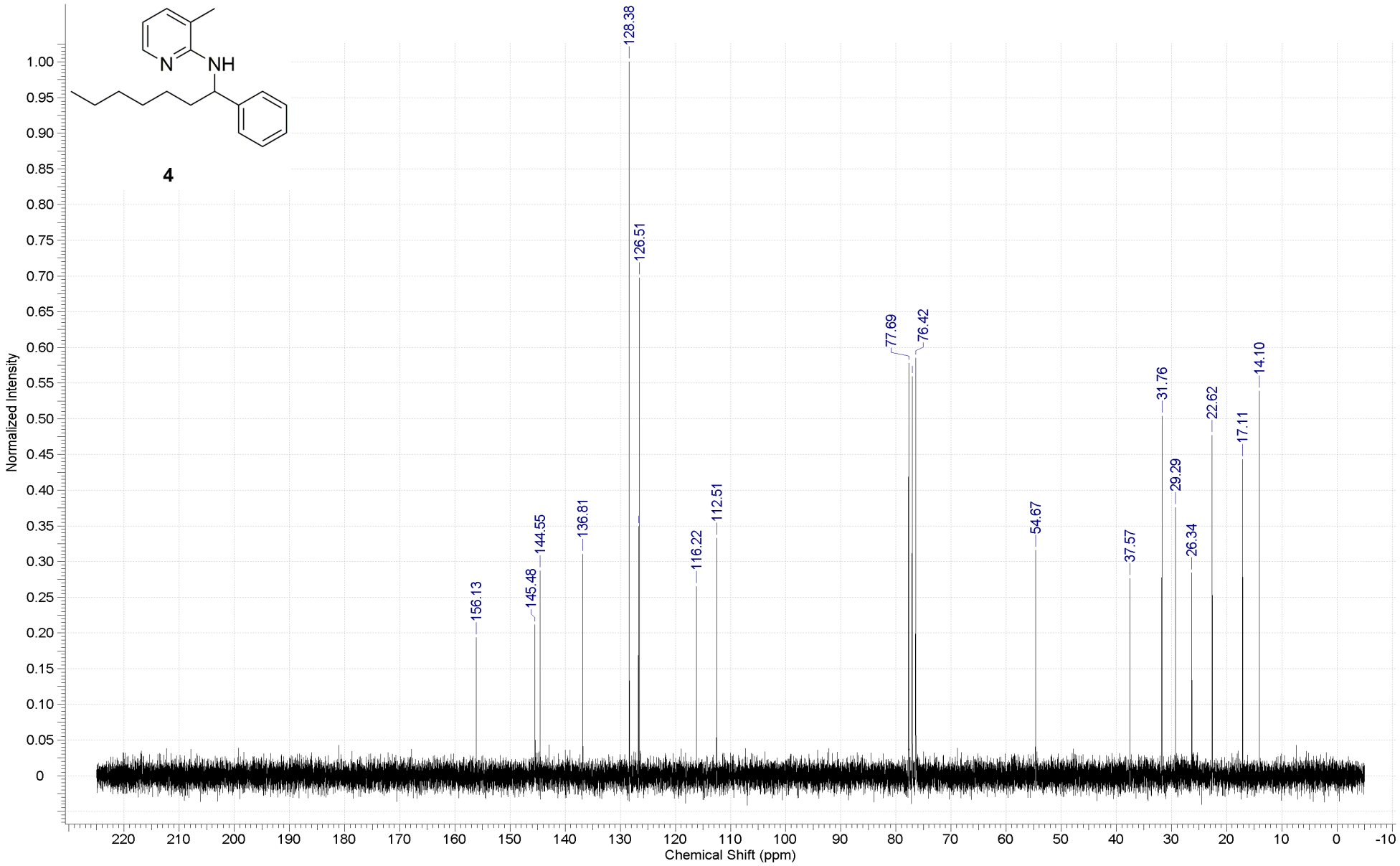
4
N
NH
128.38
126.51
77.69
76.42
156.13
145.48
144.55
136.81
116.22
112.51
54.67
37.57
31.76
29.29
26.34
22.62
17.11
14.10
Normalized Intensity
Chemical Shift (ppm)

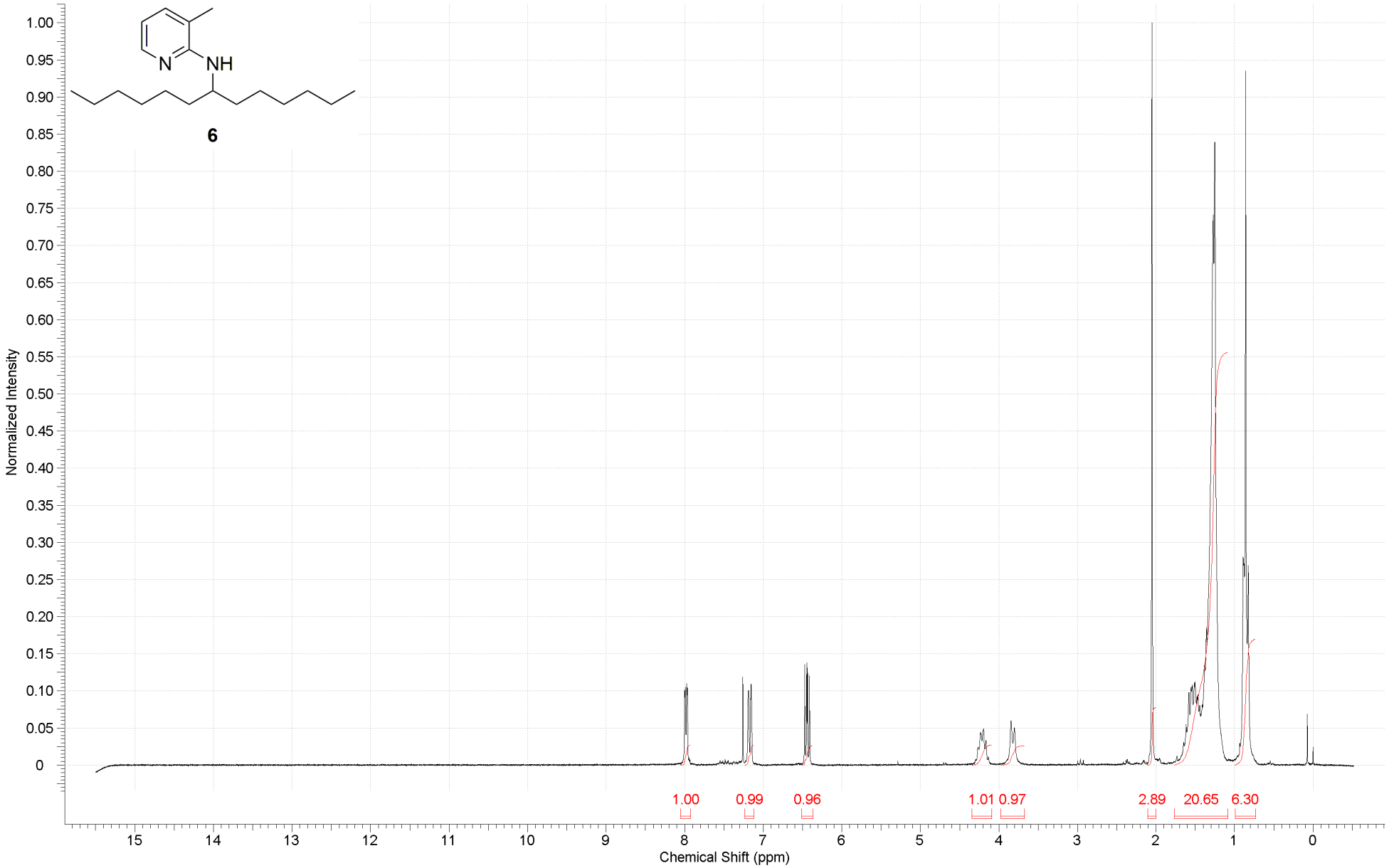
N
NH
6
Normalized Intensity
Chemical Shift (ppm)
1.00
0.99
0.96
1.01
0.97
2.89
20.65
6.30

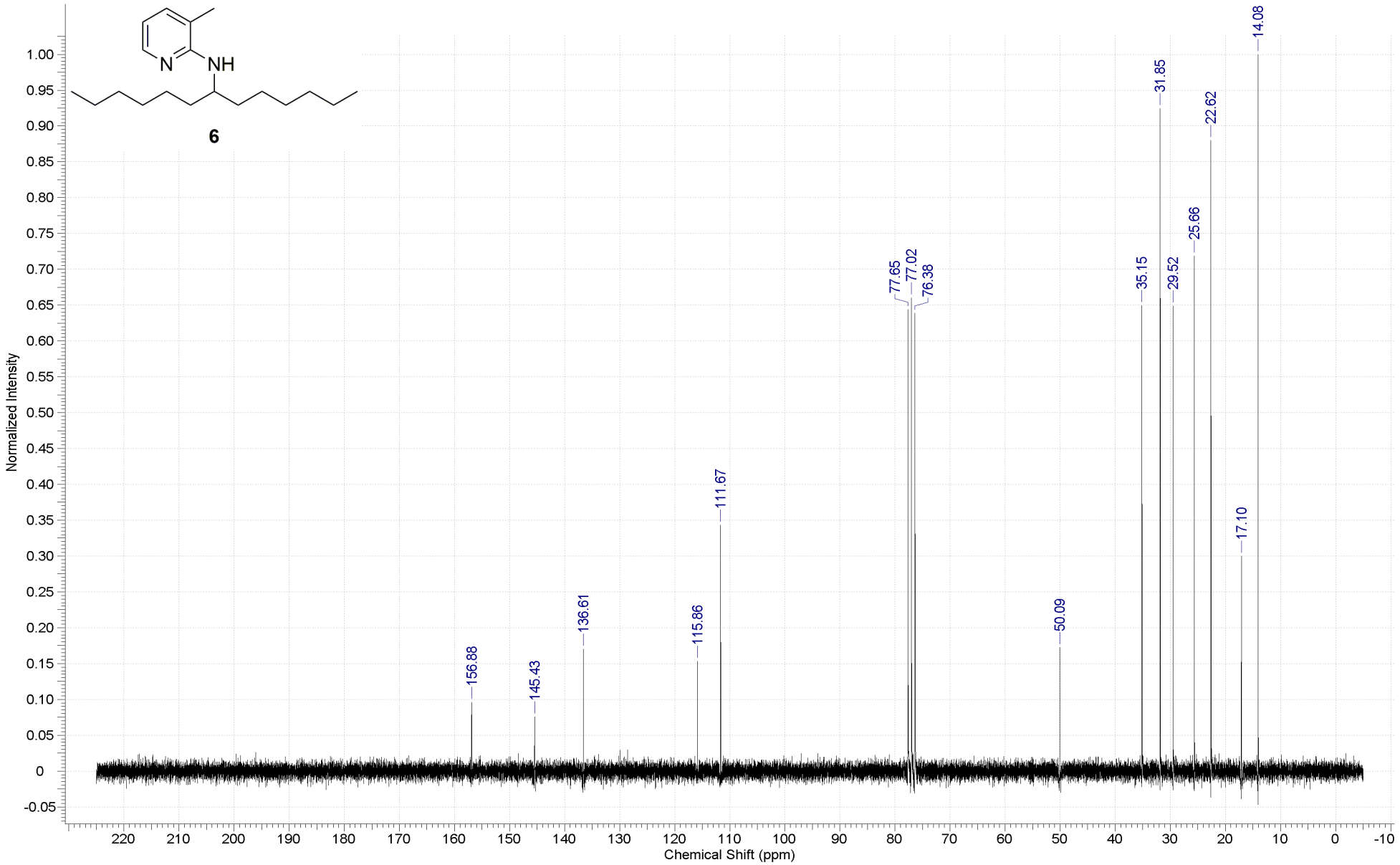
N
NH
6
Normalized Intensity
Chemical Shift (ppm)
156.88
145.43
136.61
115.86
111.67
77.65
77.02
76.38
50.09
35.15
31.85
29.52
25.66
22.62
17.10
14.08

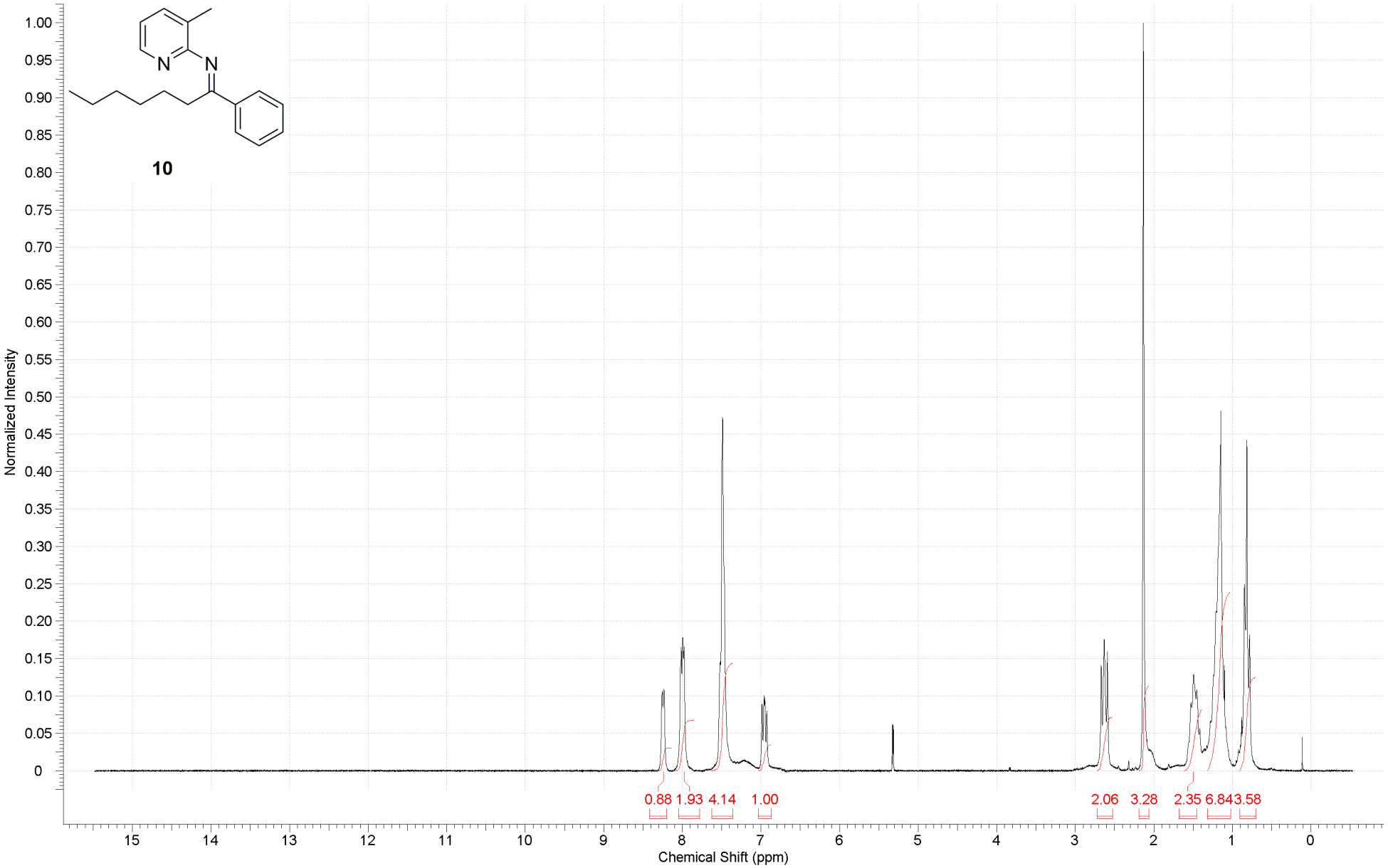
10
Normalized Intensity
Chemical Shift (ppm)
0.88 1.93 4.14 1.00
2.06 3.28 2.35 6.84 3.58

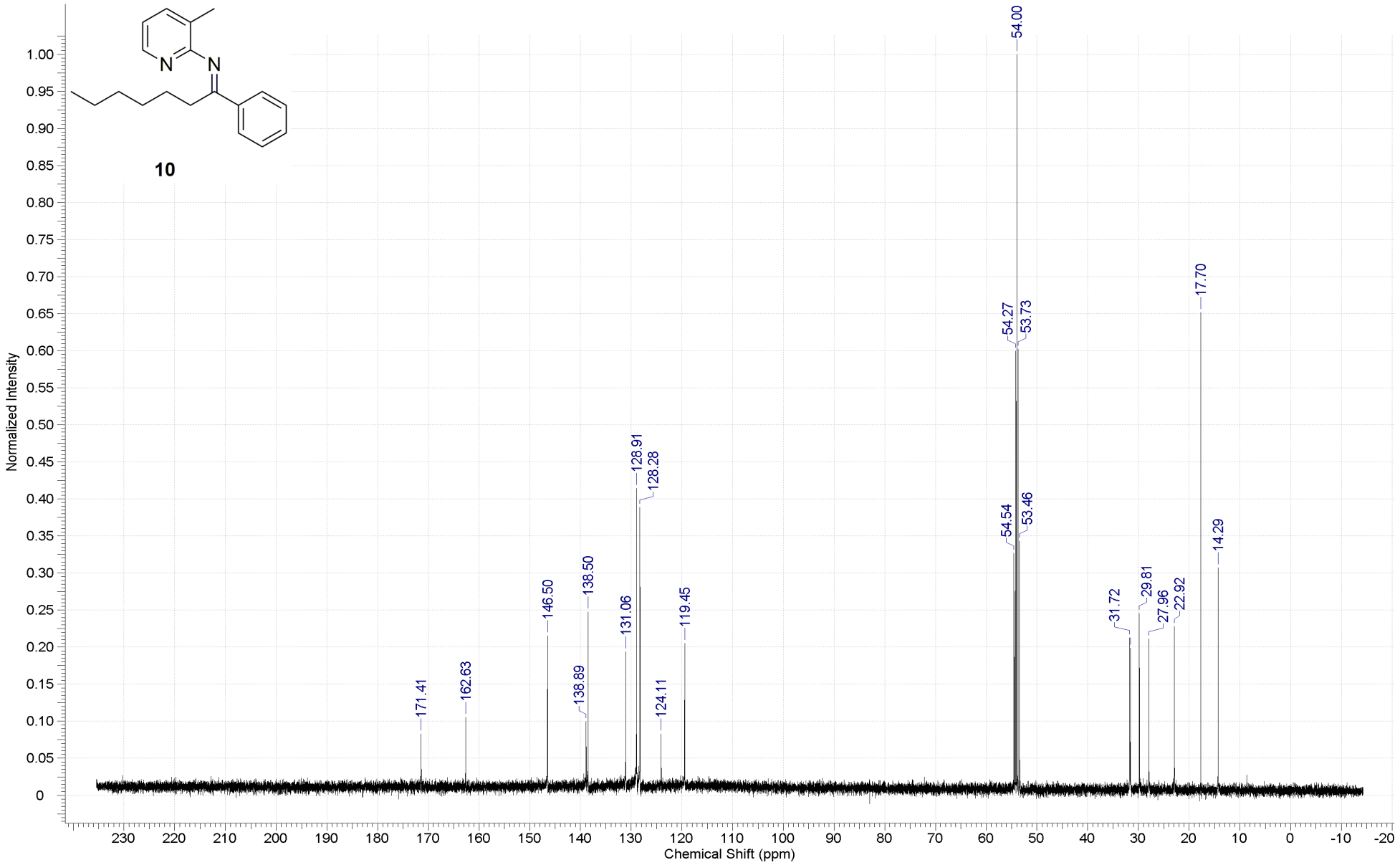
10
Normalized Intensity
Chemical Shift (ppm)
54.00
54.27
53.73
54.54
53.46
128.91
128.28
146.50
138.50
131.06
138.89
171.41
162.63
124.11
119.45
17.70
14.29
31.72
29.81
27.96
22.92